NRL REPORT 3621

PR-3624

TRANSIENT CHARACTERISTICS OF D-C MOTORS AND GENERATORS

E. L. Brancato and A. T. McClinton

January 30, 1950

Approved by:

Dr. W. C. Hall, Superintendent, Electricity Division

NAVAL RESEARCH LABORATORY

CAPTAIN F. R. FURTH, USN. DIRECTOR

WASHINGTON, D.C.

DISTRIBUTION

BuAer	1
BuShips	
Attn: Code 660	1
Attn: Code 660U	6
ONR	
Attn: Code 427	1
CNO	1
Dir., USNEL	2
CDR, Material Laboratory, New York Naval Shipyard	
Attn: C. E. Fraser, Head, Electrical Section	2
Attn: H. L. Flatt, Head, Power Section	2
CO, U. S. Naval Submarine Base, New London	
Attn: Elect. Dept.	1
CDR, USNOTS	
Attn: Reports Unit	2
BAGR, CD, Wright-Patterson AFB	
Attn: CADO-D1	1
OCSigO	
Attn: Ch. Eng. & Tech. Div., SIGTM-S	1
CO, SCEL	
Attn: Dir. of Eng.	2
Office of Tech. Services, Dept. of Commerce	2
RDB	
Attn: Library	2
Attn: Navy Secretary	1
Naval Res. Sec., Science Div., Library of Congress	
Attn: Mr. J. H. Heald	2

CONTENTS

ABSTRACT

Using a mock submarine propulsion plant, an experimental investigation has been conducted to obtain for various maneuvering conditions design data on system fault currents and to evaluate existing relations describing the transient behavior of d-c machines. The first objective has been attained and theresults have been submitted in three separate reports. The present report is concerned with the latter phase of investigation and presents oscillographic data with theoretical observations on the transient behavior of d-c machines. These observations indicate that the theoretical relations do not possess the accuracy necessary for optimum design of shipboard power systems. In general they do not adequately reflect the influence of initial conditions of load, voltage, and speed on peak currents. In addition, they are deficient in predicting, within design accuracy, the buildup and decay of armature and field circuit currents. Hence, more fundamental knowledge of the internal phenomena of rotating machinery is required before relations may be formulated tocalculate with the required accuracy the transient response of d-c machines.

PROBLEM STATUS

This is an interim report; work on this problem is continuing.

AUTHORIZATION

NRL Problem E01-05R

(BuShip's ltr. SS/60 (660U-330) dated 26 September 1947.)

NS 676-003

TRANSIENT CHARACTERISTICS OF D-C MOTORS AND GENERATORS

BACKGROUND

The Navy, having extensively used d.c. for ship's service and propulsion power plants over a long period of years, has always been vitally interested in the question of transient performance of d-c rotating machinery and the effect of the transients on system operation. Of special interest has been that phase of system study which deals with fault current analysis and the application of protective devices to the power plant. However, in the early days of small capacity plants, fault current analysis was not of major importance since the available amount of short circuit current in the system was relatively small and most of the protective devices, which had been primarily designed for shore station use, had more than adequate interrupting capacity to meet the application requirements. Thus accurate knowledge of fault currents to be expected was inconsequential. When the electrical loads on naval vessels started to increase rapidly just before World War II, with the resultant increase in generating capacity and available fault currents, system study work received new emphasis. Unfortunately, the mathematical tools available to the a-c system designer, which enable him to calculate such items as sub-transient reactances from the geometry of the machines, are not readily available to the d-c system designer. The engineers concerned with d-c system work had to satisfy themselves with rule-of-thumb methods for calculating available short circuit currents in the system, and they used excessively large safety factors in their protective devices to offset the probable inaccuracy in their system study work. In most cases, however, this worked out entirely satisfactorily because of the fact that high-interrupting-capacity protective equipment was being supplied to low-capacity power systems.

Consideration of the performance of d-c machinery under fault conditions is extremely significant in shipboard d-c systems where freedom from commutator flashover and reliable circuit breaker operation are necessary. This is especially true in the larger capacity systems where excessive fault currents cause commutator flashover and small fault currents make the attainment of circuit breaker selectivity difficult. In order to set up successfully design specifications for protective devices that will operate reliably with the rotating machinery, it is important that the application engineer have the following information:

(a) The maximum short circuit current of motors and generators in the system.

(b) The rate of rise and decay of the short circuit current of the motors and generators.

(c) Information relative to the flashover characteristics of the rotating machinery.

(d) Information relative to the effect of changes in voltage, speed, and machine loading on the short circuit characteristics of the machinery.

Various methods of calculating the transient performance of d-c machinery[1,2,3] have been investigated in an attempt to set up design specifications for a new power plant which would result in the smallest possible size of protective equipment. The results of these calculations indicated that the theories were conflicting and the mathematical manipulations too unwieldy to be of use to the application engineer. Calculated peak short current current from newly designed machines appeared to be excessive. Accordingly it was necessary to (1) obtain test data on Navy type equipment to ascertain the order of magnitude of short circuit currents for the immediate design problem and (2) check the theoretical considerations set forth in the several technical papers[1,2,3] for future work.

METHOD OF CONDUCTING THE INVESTIGATION

In order that sufficient experimental data could be obtained to fulfill these requirements relating to machine transient behavior, an existing mock submarine propulsion and auxiliary plant at the U.S. Naval Submarine Base, New London, Connecticut, was modified to adapt the system to the purpose of this study. The equipment composing the system is indicated on Figure 1. Figure 2 is a single line diagram of the power system of Figure 1 in which the resistance of cable, including contact resistance, is indicated.

Among the larger components is the propulsion generator (Figure 3), an 1100-KW machine compensated with half-turn differential compounding, separately excited; Figure 4 illustrates the diesel drive for this generator. The propulsion unit consists of two double armature motors; one is a 280-rpm motor (Figure 5), compensated, compound wound, separately excited. The second motor rated at 1300 rpm and shown in Figure 6 is coupled to the shaft of the first motor through a suitable reduction gear as presented in Figure 7.

The short-circuiting equipment was connected to the aft battery contactors of a Westinghouse control cubicle of SS228 class of vessels. This equipment consisted of a single-pole circuit breaker of 8,000 amperes, 1,000 volts rating, solenoid-operated to initiate the short circuit, and a backup circuit breaker of identical rating, except for the addition of arcing contacts to interrupt the fault current. As a safety measure, a solenoid-opened emergency single-pole knife switch was inserted in the short circuit loop to interrupt

---

[1] *Linville, T. M. and Ward, H. C., Jr., "Solid Short Circuit of Direct Current Motors and Generators," AIEE Technical Paper 49-39, December 1948.*

[2] *Linville, T. M. "Current and Torque of D.C. Machines on Short Circuit," AIEE Transactions, 65, 956-965, 1946.*

[3] *Frost, G. E. "The Short Circuit Characteristics of D.C. Generator," AIEE Transactions, 65, 394-402, 1946.*

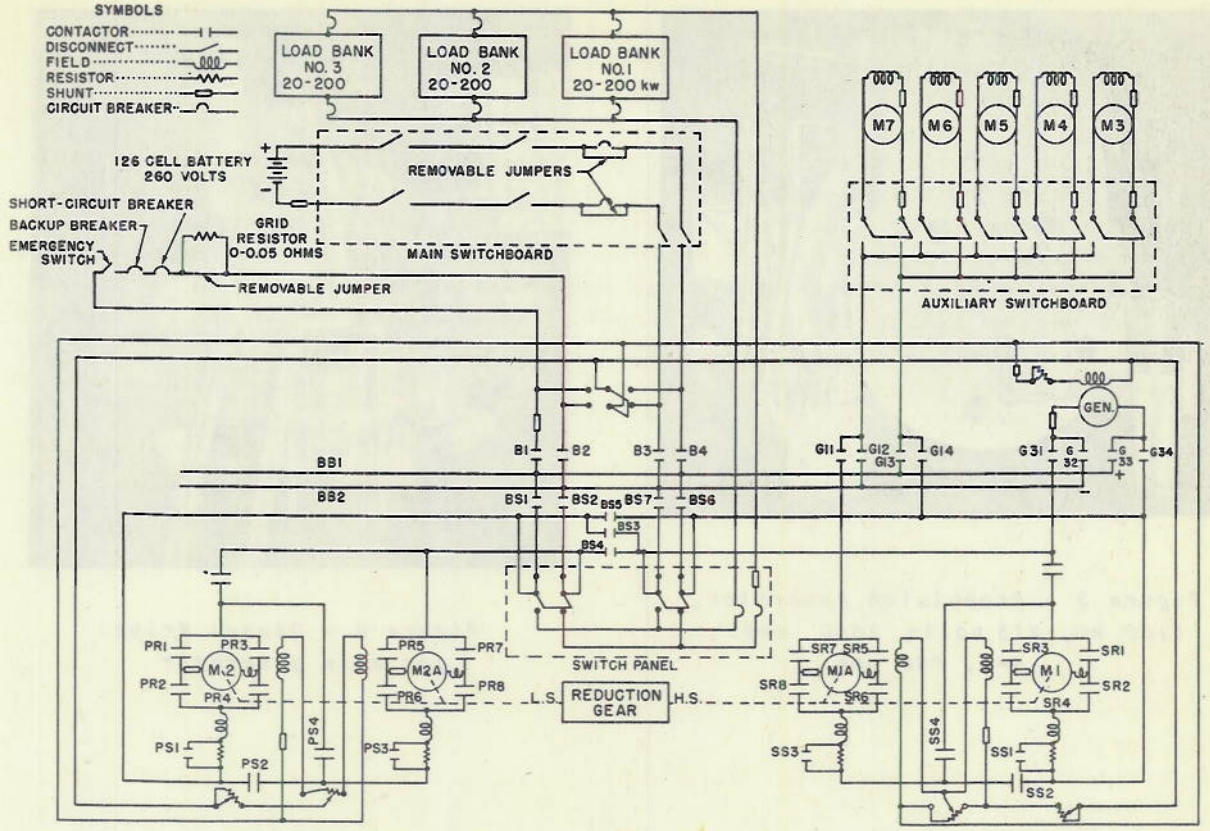

Figure 1 - Submarine mock-up, schematic diagram of power system

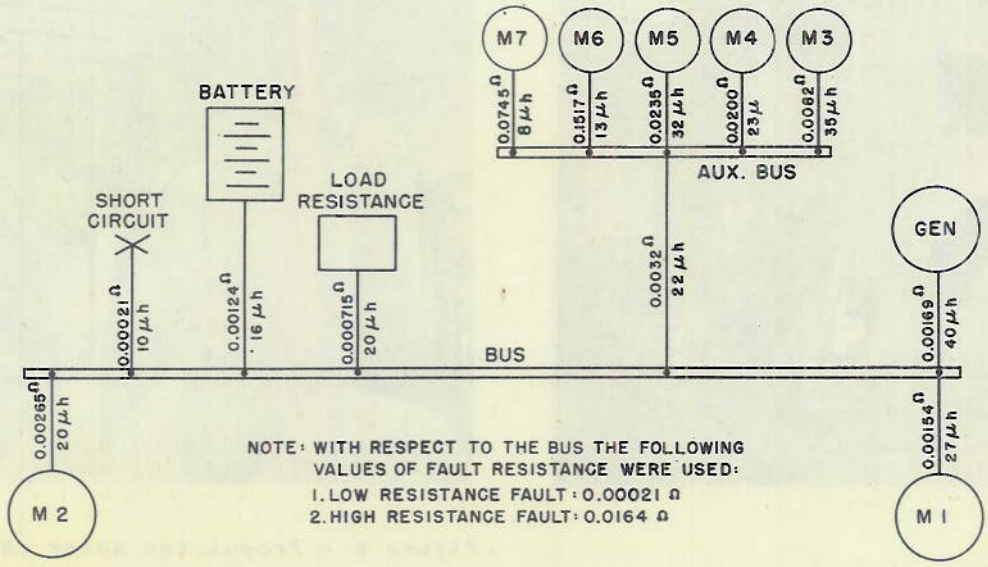

Figure 2 - Submarine mock-up, single line diagram of power system

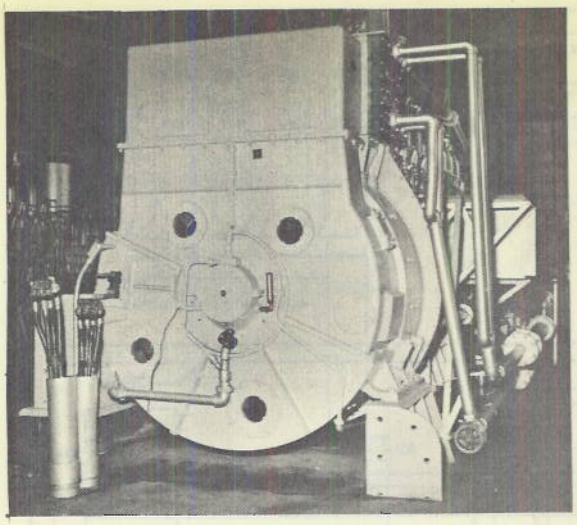

Figure 3 - Propulsion generator, 1100 kw, 415 volts, 2650 amps, d-c, 750 rpm

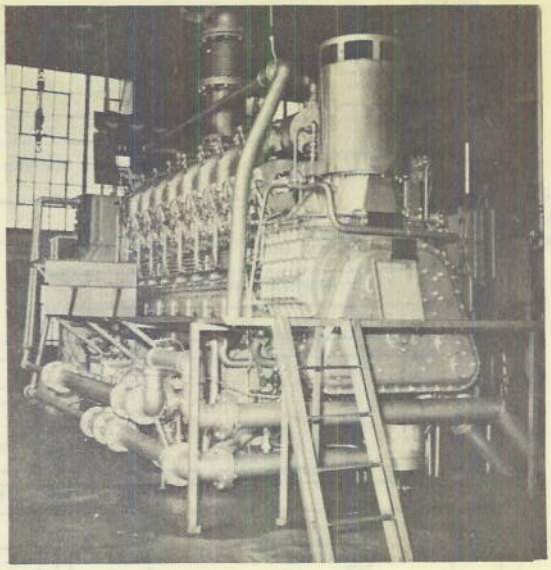

Figure 4 - Diesel drive for main generator

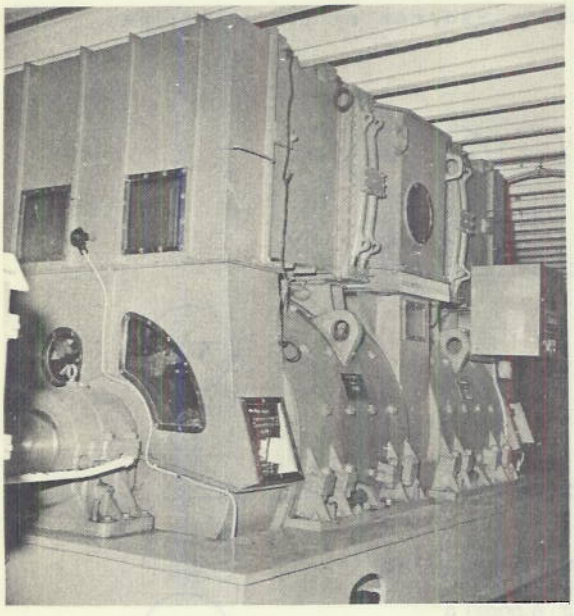

Figure 5 - Propulsion motor (M-2), 1375 hp, 415 volts, d-c, 2650 amps, 280 rpm

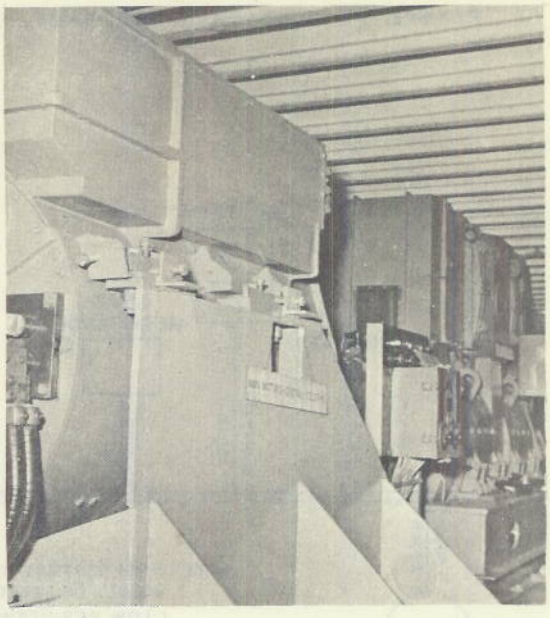

Figure 6 - Propulsion motor (M-1), 1375 hp, 415 volts, d-c, 2600 amps, 1300 rpm; motor (M-2) in the background

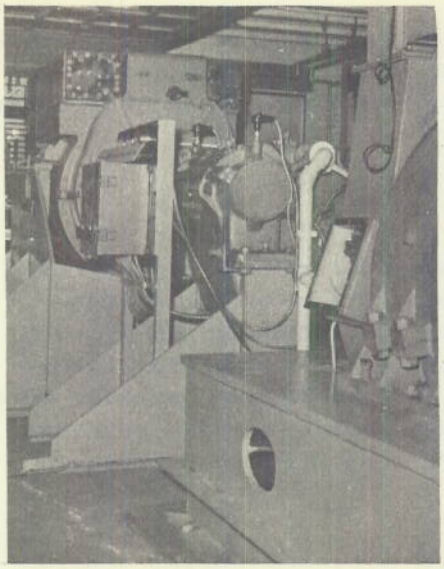

Figure 7 - Reduction gear between propulsion motors M-1 and M-2

the fault current in the event of backup circuit breaker failure. To assure that all motors and generators remained connected to the bus during the full period of short circuit, all overload protective devices were rendered inoperative. An iron grid noninductive variable resistor, of range 0 to 0.30 ohm, was installed in the short circuit loop to effect a high-resistance fault when required.

Loading was accomplished by resistance banks for the generator, by pumpback for the propulsion motors, and by auxiliaries on the smaller motors.

A synchronizing switch was developed to control the operation of those circuit breakers which initiated and interrupted the fault conditions. In addition, the switch provided the control and coordination of functions

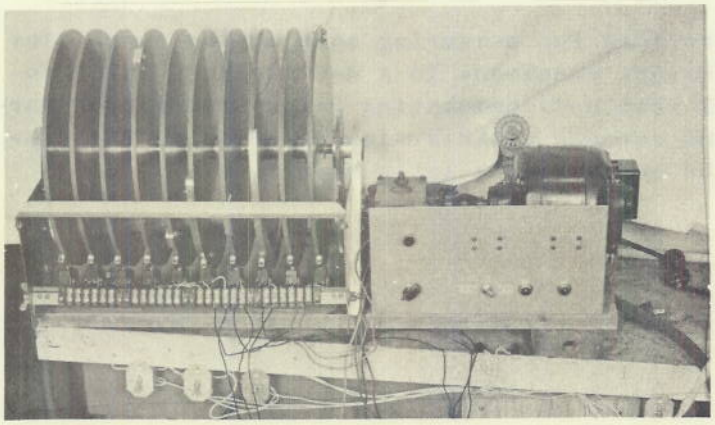

Figure 8 - Instrumentation - synchronous timing switch and metering panel

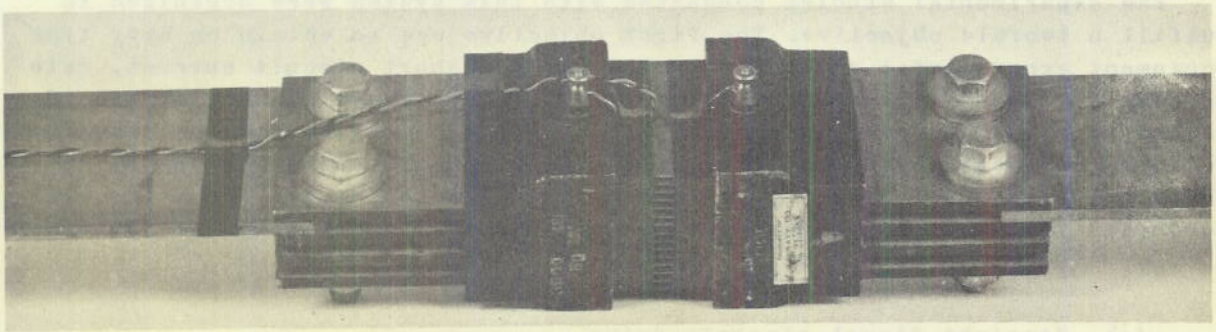

Figure 9 - Instrumentation - a typical wiring arrangement on shunt for current metering for minimum inductive pickup and intermodulation

during the period of the fault. Through the use of this device it was possible to maintain the short circuit for 0.2 second, which provided sufficient time for the current to reach peak value and start to decay. This switch may be observed in Figure 8.

Instrumentation was attained through employment of several appropriate bi-filar oscillographs in conjunction with an extensive metering system. Each metering circuit consisted of a pair of twisted conductors to prevent intermodulation of signals. These circuits terminated on a metering panel, from which they were distributed to the various oscillographs. Currents were measured by utilizing standard shunts with the lead configuration as shown in Figure 9. Such an arrangement provided satisfactory frequency response for the investigation.

The transient speed change of the rotating equipment was measured by the difference in voltage between the tachometer voltage and a fixed voltage. This difference was amplified and fed to an oscillograph element.

Instrumentation was also provided for measuring some of the quantities which describe the internal transient phenomena in a d-c machine. These include flux changes in air gap of main and commutating poles, commutator bar-to-bar voltages, brush drops, and current distribution in brushes. The discussion of these data will be the subject of a later report.

EXPERIMENTAL RESULTS

Oscillographic Data

The experimental studies conducted with this system were organized to fulfill a twofold objective. The first objective was to obtain on Navy type equipment experimental evidence for the maximum short circuit current, rate of rise and decay of current, and the way in which these quantities are affected by varying certain parameters. The second objective was to check the validity and accuracy of existing theoretical relationships for computing these quantities. In order to accomplish the first objective the study was conducted for three basic maneuvering conditions of a submarine as follows:

(a) Straight diesel electric drive

(b) Diesel electric drive with batteries on charge

(c) Submerged conditions, motors operating off the battery.

The data obtained for the above conditions have been presented during the progress of this work in three separate interim reports.[4, 5, 6] The oscillograms from which the above data were abstracted are submitted for reference purposes in Appendix II. They indicate the effect of such variables as initial speed, load, and voltage on the short circuit current.

Although these effects are discussed in detail in later paragraphs, it is of interest to observe at this time some effects not analyzed in this report, namely, flashover and compounding. At high short circuit currents a number of machines flashed over; this phenomena may be observed in Figures 34, 36, 37, and 42 for the propulsion generator: Figure 37 for the propulsion motors M-1 and M-2; and Figure 47 for the 90 h.p. motor, M-3 (See Appendix p.44). Flashover, which is a disruptive discharge around the commutator, has the effect of shunting a large portion of fault current internally, thereby reducing the current contributed to the external circuit. This is illustrated by Figure 42. In this instance the voltage drop in the arc was less than the voltage at the short circuit; therefore the machines on the system fed current into the propulsion generator. In other cases the flashover was recurrent in character, consisting of periodic establishment of flashover and recovery as illustrated by the current trace of generator in Figure 36, and of the 90 h.p. motor, M-3, in Figure 47.

The influence of cumulative and differential compounding on the magnitudes of short circuit contribution and induced transient shunt field current may be observed in Figures 40 and 41 for the propulsion motor, M-2. In a cumulative compounded machine (as a generator) two actions occur during short circuit: the direct axis component of armature reaction tends to reduce the air gap flux, while the series field tends to increase this flux. In a differentially compounded machine, however, both the armature as well as the series field tend to reduce the air gap flux. Since the flux linkages with any inductive circuit cannot be changed instantly, current is induced in the field winding approximately proportionate to the change in air gap flux. Therefore, the change in shunt field current will be greater for the differential compounded machine. On the other hand the armature current will be greater for the cumulative compounded machine since this current is directly dependent upon the air gap flux.

There are two other observations worthy of note. On a number of oscillograms it will be found that the generator was removed from the system prior

---

[4] *NRL Interim Report 3310-32/48 (or) dated 24 September 1948, Short Circuit Characteristics of Submarine Propulsion and Auxiliary Power Equipment, to BuShips.*

[5] *NRL Interim Report 3310-19/49 (or) dated 18 August 1949, Short Circuit Characteristics of Submarine Propulsion and Auxiliary Power Equipment, to BuShips.*

[6] *NRL Interim Report 3310-24/49(mc) dated 27 September 1949, Short Circuit Characteristics of a 300 KW Submarine Auxiliary Generator, to BuShips*

to the removal of the short circuit from the system. This premature removal of the generator was caused by the normal operation of the generator contactors which inadvertently had been left operative during the run. The second item of importance is the overvoltage produced from switching transients on opening of the bus circuit breaker. In some cases the overvoltage produced was as high as 350 percent of steady state. This extreme surge may be observed in Figure 31.

Equivalent Circuit

The effect of variables like initial speed, load, and voltage is best understood in the light of those factors determining the transient characteristics of a d-c machine. For this purpose use may be made of the simplified equivalent circuit. There are many elements that affect the transient response of rotating machinery. However, if for the moment only peak currents are considered, attention need be given to three factors only. These are armature circuit ohmic resistance, brush contact drop and reactance voltage, and flux reduction and distortion. By translating these quantities into an effective internal resistance, and by considering the generated voltage as a constant, the direct-current machine presented schematically in Figure 10a can be represented by the equivalent circuit of Figure 10b.

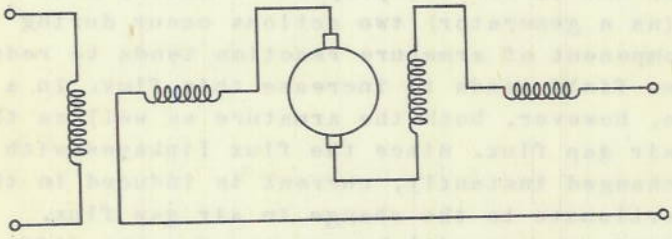

Figure 10a - Schematic diagram of d-c machine

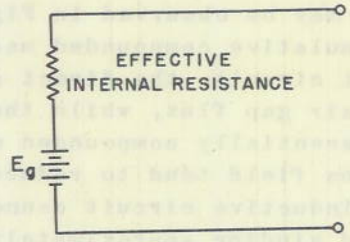

Figure 10b - Equivalent representation of d-c machine

This circuit has been selected in displaying the characteristics of the several machines considered. It should be noted, however, that this circuit is applicable only for the computation of peak values of short circuit current for individual machines or for the total value of several in a system. Reasonable accuracy can be expected in a system calculation if the time to reach peak current is essentially equal for all machines on the system and if the effective internal resistance is accurately known. Where the transient of the currentis desired, a more nearly complete representation of the machines with an equivalent circuit will be required. Such a circuit would require resistance and inductances to represent the armature and field circuits, but the required accuracy of calculations would have to justify the necessarily elaborate computations.

Machine	Rated Voltage (Volts)	Rated Speed (RPM)	Rated Current (Amps)	Current Rise Amps/Sec X10^6	Internal Resistance (Ohms)	Zero Resistance S.C. Current (Per Unit) (Calculated)
Generator	415	750	2650	2	0.019	8.5
Generator	345	1200	870	1.43	0.0355	12.0
Motor	415	1300	2650	2.5	0.021	7.5
Motor	415	280	2650	2.5	0.032	5.0
Motor	250	1750	298	0.2	0.085	10.0
Motor	250	550	176	0.04	0.170	8.5
Motor	250	1600	73	0.04	0.360	9.5

Figure 11 - Short circuit constants of machines for operation at normal full-load ratings

Figure 11 presents values of effective internal resistance and generated voltage found for several machines by laboratory tests. The values shown in this table are for operation at rated conditions prior to application of the fault. Discussion to follow will indicate the effect of such factors as speed, load, and voltage on these equivalent values.

Effective Internal Resistance Variation

The experimentally obtained transient resistances are plotted in Figures 12 through 14 against the parameters of load, speed, and voltage. Referring to Figures 14 and 15, it is noted that the magnitude of load prior to short circuit has a sizeable influence on the resulting peak short circuit currents or effective internal resistance, and that the peak current increases and resistance decreases with increasing load. The reason for this behavior is not evident, although it is suspected that higher resistance in the field circuit at lower loads may result in a quicker deterioration of flux linkages, which in turn may augment the reduction in air gap flux beyond that anticipated from the increase of leakage flux during transient loading. A comparison of the percentage decrease in internal resistance between a lightly differential-compounded machine (Figure 12) and a more heavily differential-compounded machine of Figure 13 tends to verify this statement. It can be noted that the percentage increase in field circuit resistance, between full load and no load, and the increase in transient field current due to transformer action of the armature circuit during a short circuit, is smaller for a lightly compounded than for a heavily differential-compounded machine. Thus the change in the rate of destruction of flux linkages for a change of load from full load is higher in the heavily differential-compounded machine. By this token, it is expected that the magnitude of short circuit currents from a cumulatively compounded machine would not be unduly influenced by the initial load.

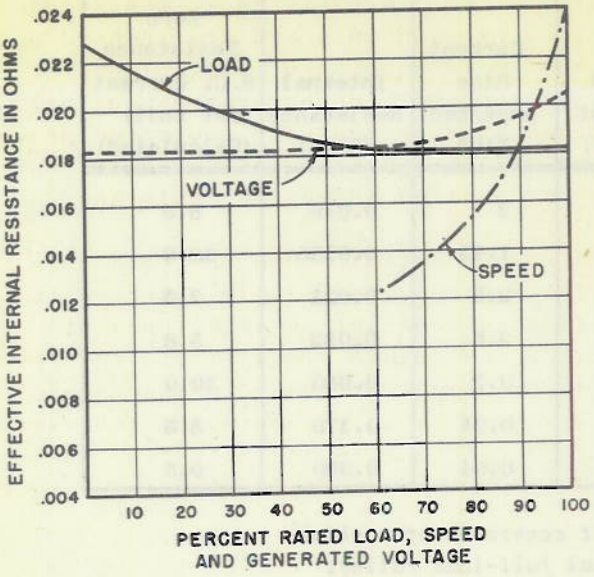

Figure 12 - Effect of initial operating conditions on effective internal resistance (1100-kw, 415-volt, 750-rpm generator)

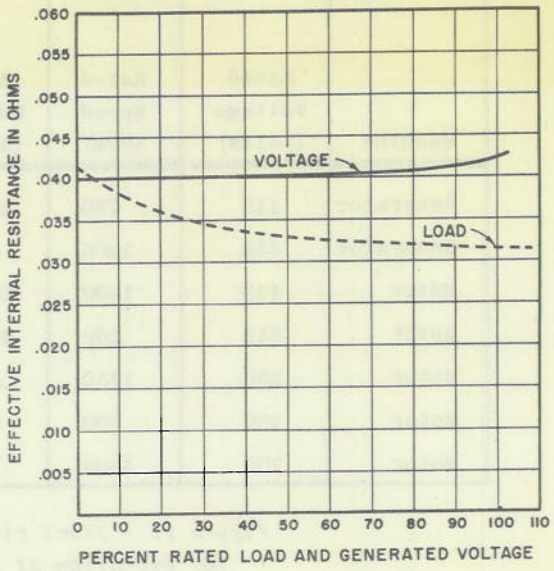

Figure 13 - Effect of initial operating conditions on effective internal resistance (300-kw, 345-volt, 1200-rpm generator)

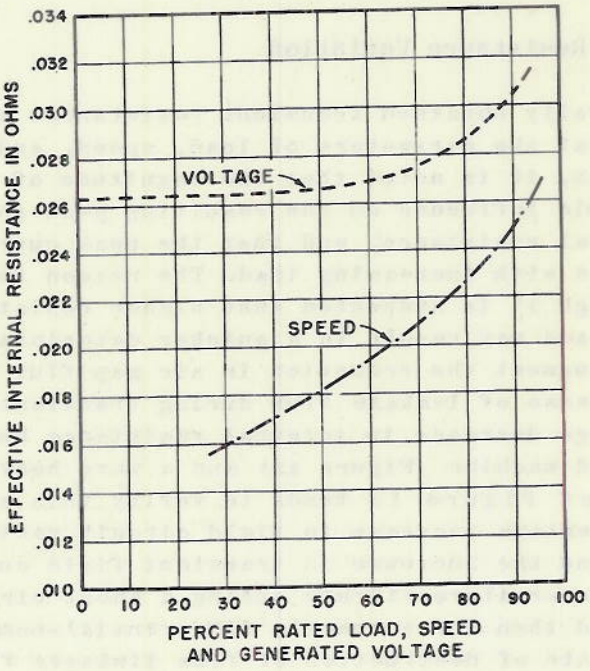

Figure 14 - Effect of initial operating conditions on effective internal resistance (1375-hp, 415-volt, 280-rpm motor)

The speed also influences the machine effective resistance. The speed characteristics were obtained for the two large machines and are graphed on Figures 12 and 13. The effect of speed change is consistent for all units, that is, the internal resistance rises and the peak current correspondingly decreases with increasing speed. This trend is expected, for the speed proportionally affects the reactance voltage which, appearing as an equivalent brush drop, contributes to the magnitude of machine effective resistance.

If the machine effective resistance were constant, then the peak current would increase with the generated voltage. However, it is observed in Figures 12, 13, and 14 that this resistance is constant up to 50 percent voltage, but above this voltage the machine resistance rises. It is inferred that this effect is due to an increase in leakage flux owing to increased saturation of the pole iron. In addition, there is an accompanying increase in reactance voltage, since the crowding of the flux in the pole tips increases the steepness of the flux distribution curve at the neutral point and results in a decrease in commutation time.

The behavior of a machine, relative to short circuit contribution, when operating as a motor or as a generator, is of practical interest. Two motors were operated, each as generator and as motor, at similar load, voltage, and speed conditions. Referring to Figure 15, it is noted that the peak short circuit current is less for motor action than for generator action and that this difference in current decreases asthe initial load is decreased.

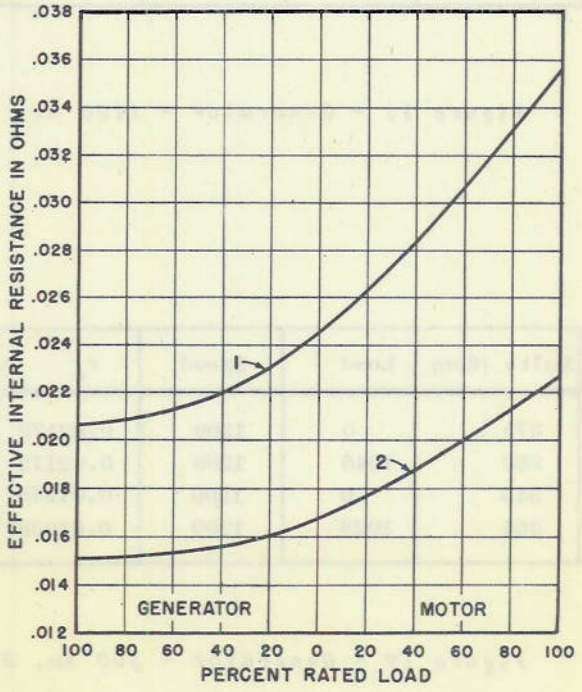

Figure 15 - Effect of change from motor to generator action as initial condition on effective internal resistance

(1) 1375-hp, 415-volt, 1300-rpm motor
(2) 1375-hp, 415-volt, 280-rpm motor

THEORETICAL OBSERVATIONS

Peak Short Circuit Current

In an attempt to verify the validity of existing theory relating to short circuit characteristics of d-c machines, calculations of peak short circuit currents were made for thefault conditions towhich these machines have been subjected. The method ofcalculation is outlined in Appendix I. The results of these computations are embodied in Figures 16 through 19. These tables outline the pertinent conditions and resistances and compare the calculated values to the actual test results.

Volts (Gen)	Load	Speed	r_e	r_d'	$I_{Calc.}$	I_{Test}	Percentage
428.8	2300	715	0.2407	0.3557	2.91	3.09	94.2
427.3	2000	715	0.01450	0.13085	7.86	7.02	112.0
415.0	0	715	0.01213	0.12667	7.89	7.74	102.0
314.1	2600	715	0.01448	0.12657	5.97	5.70	104.7
214.2	2400	715	0.01453	0.12407	4.15	3.92	105.6
116.9	850	619	0.0152	0.1126	2.50	2.41	103.7
116.7	800	428	0.0150	0.0936	3.00	3.02	99.5
206.6	1200	715	0.0142	0.1258	3.96	3.77	105.0
204.8	600	715	0.0148	0.1241	3.98	3.47	104.5

Figure 16 - Generator - 1100 kw, 415 volts, 2650 amperes, 750 rpm

Volts (Gen)	Load	Speed	r_e	r_d'	$I_{Calc.}$	I_{Test}	Percentage
270	0	1200	0.02172	0.21261	4.88	5.07	96.4
283	1045	1200	0.02172	0.21241	5.125	6.71	76.4
345	0	1200	0.01238	0.1315	7.6	8.45	90.0
365	1028	1200	0.01238	0.1325	7.99	10.52	76.0

Figure 17 - Generator - 300 kw, 345 volts, 870 amperes, 1200 rpm

Volts (Gen)	Load	Speed	r_e	r_d'	$I_{Calc.}$	I_{Test}	Percentage
209	1900	950	0.01235	0.09753	5.17	6.30	82.1
205	1700	1240	0.01229	0.11409	4.34	5.70	76.2
134	1800	718	0.01450	0.0696	4.63	4.71	98.3
133	1720	418	0.01430	0.0714	4.52	4.97	91.1
122	1600	718	0.01203	0.06714	4.36	5.70	76.5
122	1800	450	0.01197	0.06026	4.87	5.20	93.6
*230	2470	1300	0.01660	0.1221	4.53	3.65	124.2
*247	100	1300	0.01490	0.1205	4.95	4.88	101.4
256	1725	1300	0.01415	0.1055	5.16	5.64	91.6

* Generator action prior to short circuit

Figure 18 - Motor - 1375 hp, 415 volts, 2600 amperes, 1300 rpm

Volts (Gen)	Load	Speed	r_e	r_d'	$I_{Calc.}$	I_{Test}	Percentage
394	2600	270	1.065	1.2101	0.785	0.679	115.5
390	2700	267	0.0231	0.1672	5.62	4.15	135.4
279	2400	267	0.02304	0.16277	4.13	3.43	120.3
173	2400	267	0.02375	0.15918	2.62	2.15	121.8
148	2450	91	0.02546	0.11984	1.82	1.25	145.5
88	2650	92	0.02529	0.10307	2.06	1.64	125.5
*253	1745	280	0.02323	0.1659	3.68	4.0	92.0
247.4	100	280	0.0249	0.16738	3.56	3.23	110.0
.237	2300	280	0.02674	0.1709	3.34	2.15	155.3

* Generator action prior to short circuit

Figure 19 - Motor - 1375 hp, 415 volts, 2650 amperes, 280 rpm

A review of this comparison convinces one that the relations employed in Appendix I require further improvements.

These improvements may result only from the acquisition of a more fundamental knowledge of the machine internal transient phenomena. Hence this work is being continued along the theoretical approach with this objective in mind. The factors of internal and external ohmic resistance, decay in air gap flux, and the development of a reactance voltage opposing the generated e.m.f. are considered to be all the variables that enter into the calculation of short circuit currents. However, the weighting of these effects in the proportions occurring in a d-c machine may not be accurately expressed by the existing relations.

This observation is illustrated by a set of experimental characteristics on the 1100-KW generator which are plotted in Figure 20 and compared with a corresponding set of computed characteristics. These curves attempt to demonstrate graphically the relation of peak short circuit currents developed with variations of operating conditions of load, speed, and generated voltage.

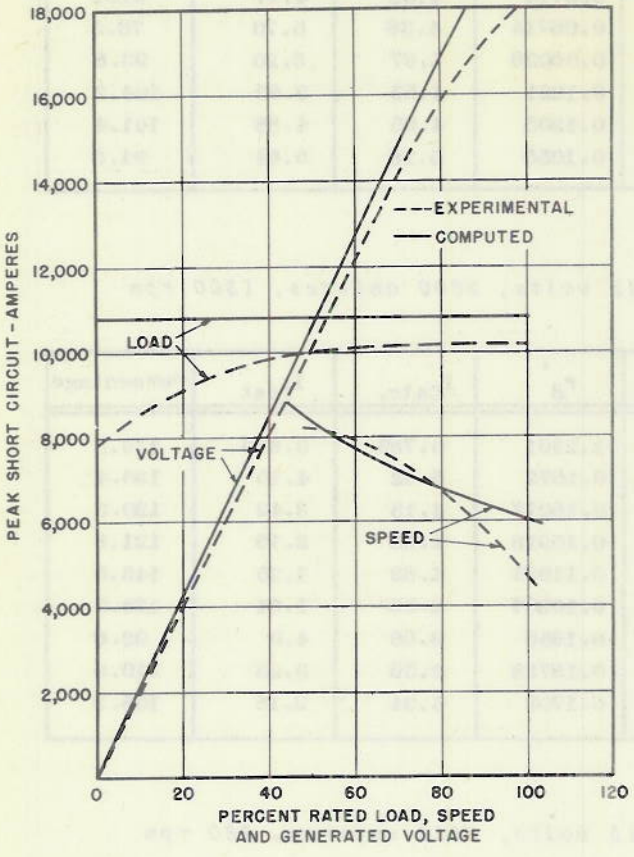

Figure 20 - Comparison of computed and experimental data onpeak short circuit current (1100-kw, 415-volt, 750-rpm generator)

Focusing attention on the curves showing the effect of load, it is observed that the peak short circuit current is a function of preshort circuit current, while the calculated values are entirely independent of initial load. There is no factor in the equations which directly recognizes the effect of load, yet a change in load from zero to 50 percent raises the peak current by approximately 20 percent, a factor that cannot be neglected even in an approximation.

Referring to the effect of voltages, it will be recalled that the effective resistance of a machine is independent of generated voltage for voltages below 50 percent, and above this value it rises appreciably. The equations involve the voltage only in the flux reduction factor, r_x', for uncompensated or partially compensated machines. Although the increase in the effective resistance of this machine, from half to full voltage, is 30 percent, the calculated rise in value for r_x' over the same region is only 10 percent. As r_x' is one of the three factors embraced by the effective internal resistance, r_d', while

the other two are independent of voltage, it is evident that the effective resistance is inadequately influenced by the change in the calculated r_x' with voltage.

In comparing the experimental to the calculated curves showing the effect of speed, it is observed that the calculated values describe a nearly straight line relation; the experimental values, although following the same trends, indicate a sharper decrease in peak current with speed, at the larger magnitudes of speed. The calculated effect of speed is apparently insufficiently descriptive of the physical behavior of the machine. The speed enters in the calculations of the reactance voltage factor, r_b', and the flux reduction factor r_x', as a linear function, except at very low speeds where the correction factor for distribution of current in the brush face becomes appreciable when calculating r_b.

Transient Armature Current

A second consideration, equally as important as computation of peak short circuit current, is the prediction of rate of rise and decrement of the transient current. The accuracy with which the rate of rise can be predicted has been demonstrated by test and calculation to be as accurate as the computation of armature inductance for conditions prior to the short circuit. Curves 1 and 6 of Figures 21 and 22, and curves 1 and 5 of Figures 23 and 24 indicate the agreement between computed and experimental data.

The calculation of the complete transient build-up is difficult to achieve due to the effect of saturation, change of flux linkages, and reduction in generated voltage during the current rise. It has been proposed that the assumption should be made that the time constant of the armature circuit be decreased by two-thirds as the armature current reaches its peak value.[7] Experimental evidence indicates that this represents too great a decrease in inductance. Results presented in Figures 21 and 22 show that for these machines the inductance decreased approximately 50 percent as indicated by curve 3, whereas data shown in Figures 23 and 24 indicate that the oscillographic trace can be more nearly duplicated with a curve representing a fixed value of armature inductance. However, such an assumption is basically incorrect since the rate of rise at any point on the curve is influenced by the voltage as well as the inductance at the corresponding interval. Thus a procedure which recognizes only an inductance change is incomplete.

The remaining portion of the transient, that is the decay of current after peak value, is associated with the shunt field circuit and its time constant. Accurate measurement of this time constant is difficult to achieve because of the necessity of duplicating the saturation of the armature and pole faces and distortion of field flux that accompany the high armature currents under short circuit conditions. Therefore the shunt field inductance was computed on the

---

[7] *Linville and Ward, op. cit.*

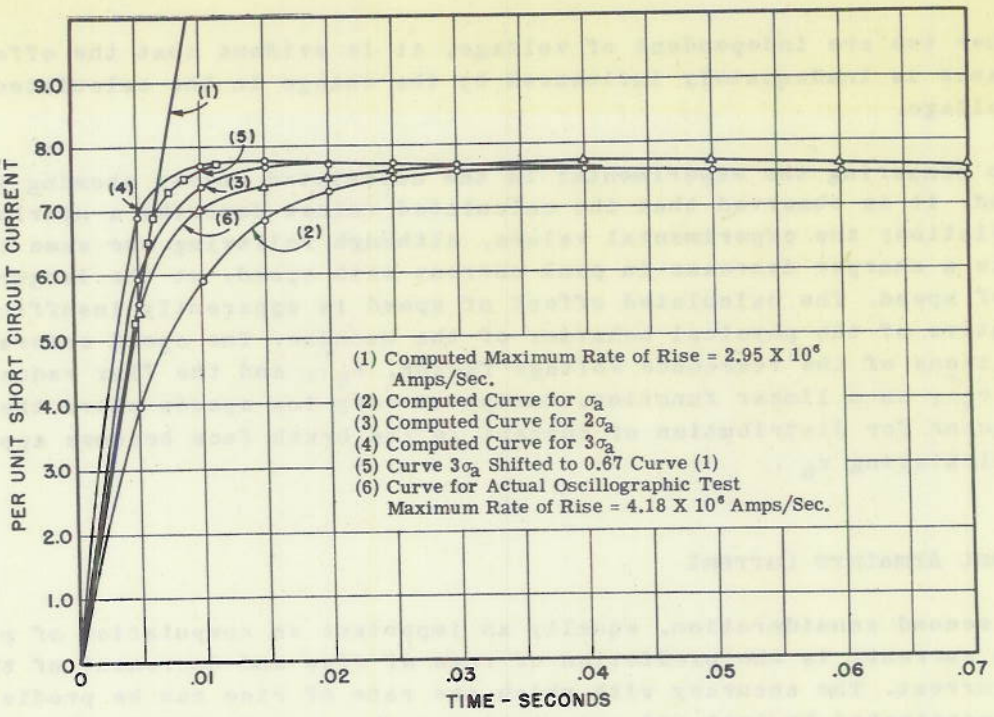

Figure 21 - Computed transient short circuit current (1100-kw, 415-volt, 750-rpm generator)

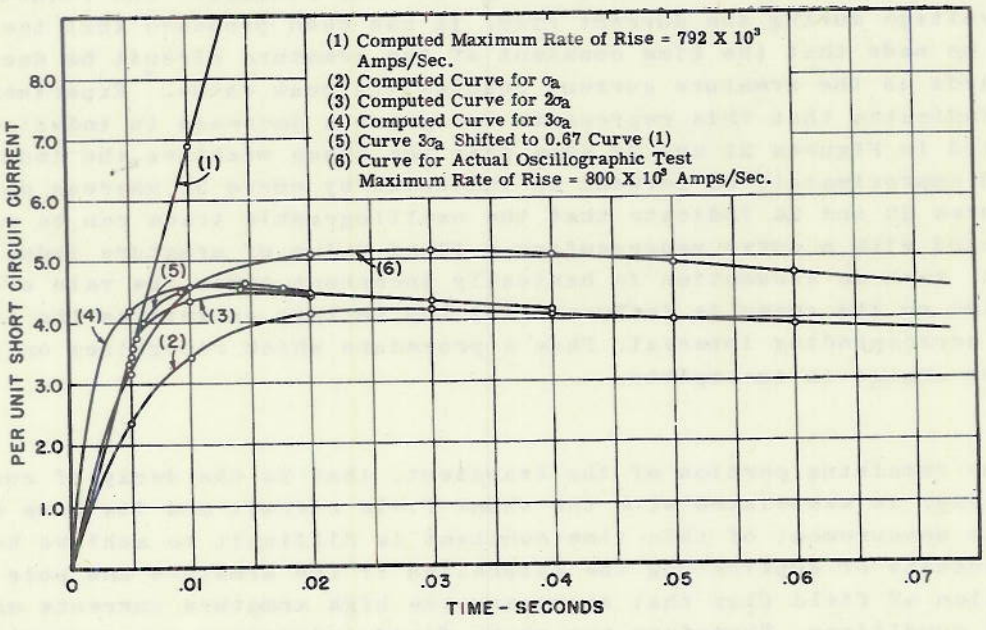

Figure 22 - Computed transient short circuit current (300-kw, 345-volt, 1200-rpm generator)

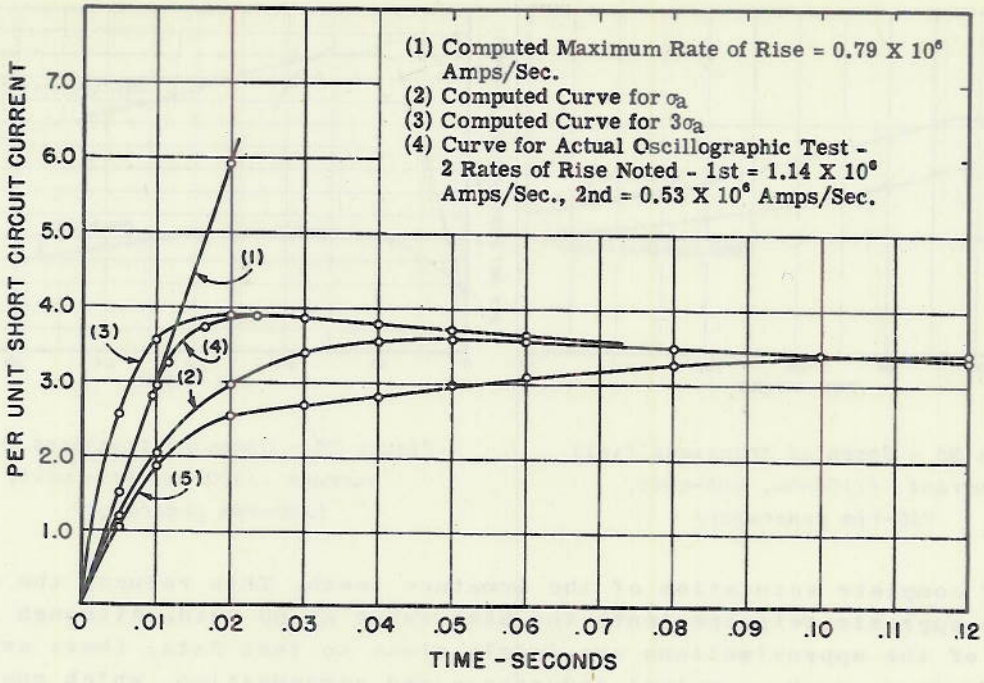

Figure 23 - Computed transient short circuit current (1375-hp, 415-volt, 280-rpm motor)

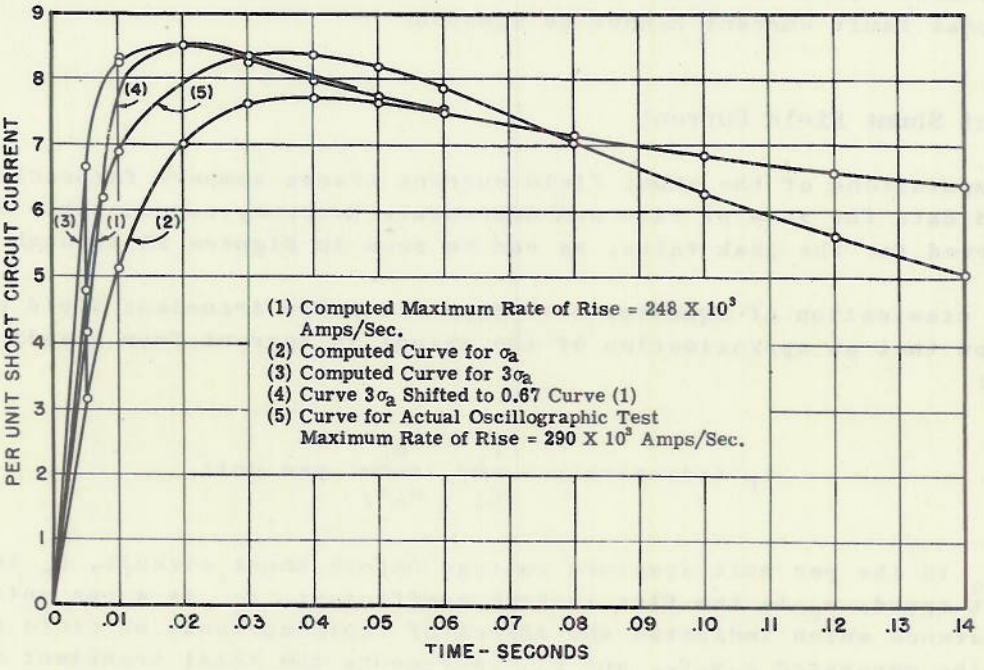

Figure 24 - Computed transient short circuit current (90-hp, 250-volt, 1750-rpm motor)

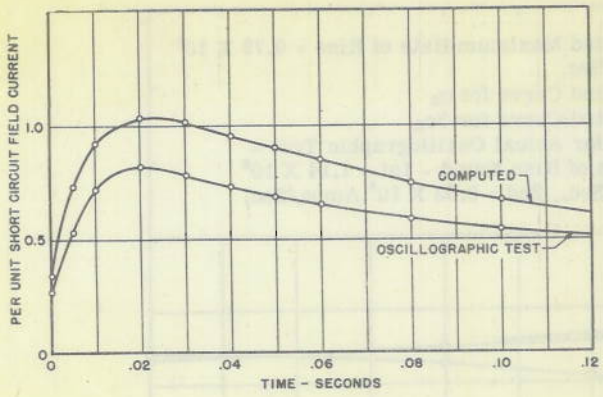

Figure 25 - Computed transient field current (1100-kw, 415-volt, 750-rpm generator)

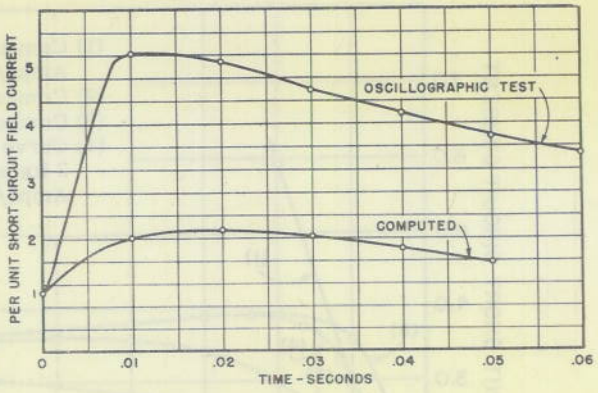

Figure 26 - Computed transient field current (300-kw, 345- volt, 1200-rpm generator)

basis of complete saturation of the armature teeth. This reduces the inductance to approximately one-tenth the base value at no load. Although the results of the approximations are fairly close to test data, there are additional factors, such as mutual inductance and compensation, which must be considered. It is important that accurate predictions of the shunt field inductance be possible since this factor can materially influence the peak value of short circuit current as evidenced from Figure 24. The computed value of peak current without giving consideration to this decrement is 9.27 per unit, whereas this becomes 7.74 per unit when the decay of the shunt field is considered. Thus it becomes evident that the influence of the shunt field on the peak fault current cannot be ignored.

Transient Shunt Field Current

Computations of the shunt field current traces compare favorably with observed data for rate of rise and decrement. However, considerable difference is observed for the peak value, as can be seen in Figures 25 through 28.

An examination of equation 8 in Appendix I for transient field current will show that an approximation of the change in current from steady state will be:

$$i_f \text{ (transient)} = \frac{r_x'}{r_d'} \cdot \frac{e_o}{n_o n_f} \text{ per unit,}$$

where e_o is the per unit armature voltage before short circuit, n_o is the per unit speed, n_f is the flux leakage coefficient, r_x' is a per unit value of resistance which indicates the effect of fault currents on field flux producing the generated e.m.f., and r_d' represents the total transient resistance. This equation shows that the per unit increase in field current is a function of the reduction in net air gap flux.

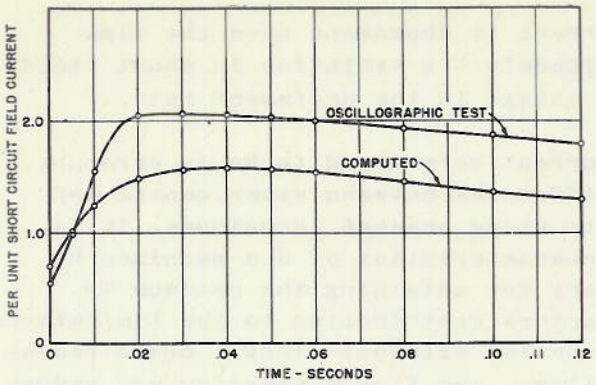

Figure 27 - Computed transient field current (1375-hp, 415-volt, 280-rpm motor)

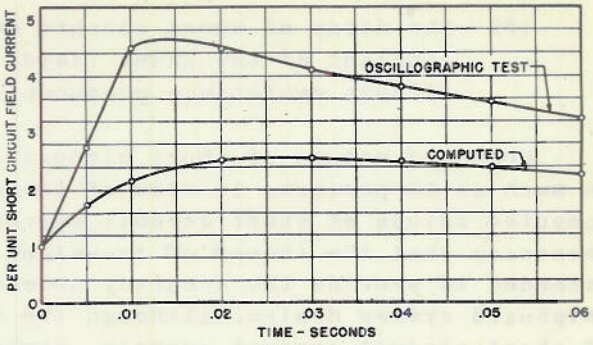

Figure 28 - Computed transient field current (90-hp, 250-volt, 1750-rpm motor)

Consideration of the term r_d' used in computing the curves of Figures 25 through 28 shows that it is in error by no more than 20 percent, whereas the oscillograph trace of field current is approximately 230 percent of the computed value. This leads to the observation that the possible flux change is greater than that predicted by r_x'. As has previously been noted, proper application of the constant flux linkage theorem may increase this term to a larger value. Two other factors that may require consideration are the coupling between the series and shunt field, which is not adequately covered by the equation, and the leakage coefficient n_f.

CONCLUSIONS

The maximum values of short circuit current with rates of rise and decay for d-c machines, as presented in detail in three earlier NRL reports, are summarized in Figure 11. In general the effects of such variables as load, speed, voltage, and compounding are as follows:

(a) Increasing the initial load on a generator will increase the short circuit current and rate of rise of current.

(b) A generator will deliver greater short circuit current than a motor of comparable design.

(c) Increasing the initial speed decreases the short circuit current but has no significant effect on the rate of rise of current.

(d) Increasing the initial generated voltage increases the short circuit current and the rate of rise of current.

(e) The short circuit current from a generator connected differential-compound will be less than that from the generator connected cumulative-compound.

(f) The decay of short circuit current is dependent upon the time constant of the shunt field. Therefore a variation in shunt field circuit resistance produces a change in the decrement rate.

Computed values of short circuit current were found to be in error by as much as 45 percent. In view of the difference between experimental and computed values of short circuit currents using present techniques, it is necessary that the theory of transient characteristics of d-c machines be extended to provide the accuracy necessary for attaining the optimum in shipboard system design. Although the factors contributing to the limitations of short circuit current (namely, armature and external circuit ohmic resistance, brush contact drop, reactance voltage, and flux distortion and reduction) have all been considered, the application of these in calculating transient response from machine constants appears inadequate. The analysis of the transient response must include the factors that will show the variation in initial load and voltage, establish a more nearly complete analysis to illustrate the magnitudes of flux change and distortion, and possibly take cognizance of the fact that the generated voltage is a variable during the transient.

The large number of factors that enter into the transient response of a d-c machine under short circuit conditions is very significant. As a result, the development of suitable relationships for armature and field currents appears to be difficult. Additional work is being done to secure an accurate measure of the internal phenomena associated with this condition. At the same time, results of the study are being correlated with system performance studies to assure completion of a theoretical approach that will be applicable to this over-all problem of system analysis under transient conditions.

* * *

APPENDIX I

EQUATIONS FOR SHORT CIRCUIT CALCULATIONS

The relations derived by Linville[8] and employed in making the calculations of transient current are as follows:

Peak short circuit current:

$$I_a' = \frac{e_o}{r_d'} \quad . \tag{1}$$

Effective internal resistance:

$$r_d' = r_w + r_b' + r_x' \quad . \tag{2}$$

When external circuit resistance is considered, it is added to r_d'.

Reactance voltage and brush drop factor:

$$r_b' = n_o E_r b \left(\frac{\varepsilon^x + 1}{\varepsilon^x - 1} \right) + V_c, \tag{3}$$

where $x = \frac{n_o E_r b}{V_c}$.

Flux reduction factor:

For fully compensated machines:

$$r_x' = \frac{K_3 n_f n_o}{1 + n_f} \quad . \tag{4}$$

For partially or uncompensated machines:

$$r_x' = \frac{10 n_f e_o + n_f (K_1 + 10K_2)(10K_3 n_o - e_o)}{100 (n_f + K_2) + 10K_1} \quad . \tag{5}$$

---

[8] *Linville and Ward, op. cit.*

Transient current:

$$i_a = \frac{e_o}{r_d} - \frac{e_o}{r_d'} \varepsilon^{-\sigma_a t} + e_o \frac{r_d - r_d'}{r_d r_d'} \varepsilon^{-\sigma_f t} . \tag{6}$$

Maximum rate of rise:

$$\frac{di_a}{dt} = \frac{e_o \sigma_a}{r_d'} . \tag{7}$$

The transient field current:

$$i_f = \frac{e_o}{n_o} \left[1 + \frac{r_x}{r_d' n_f} \left(\varepsilon^{-\sigma_f t} - \varepsilon^{-\sigma_a t} \right) \right] . \tag{8}$$

Steady-state effective resistance:

$$r_d = r_w + r_b + r_x \tag{9}$$

When external circuit resistance is considered, it is added to r_d.

For uncompensated machine:

$$r_x = \frac{10 e_o + n_o \left(10 K_3 - \frac{e_o}{n_o} \right) \left(K_1 + 10 K_2 \right)}{100} . \tag{10a}$$

For compensated machine:

$$r_x = \frac{e_o + n_o \left(10 K_3 - \frac{e_o}{n_o} \right)}{10} , \tag{10b}$$

where

$$K_1 = \frac{P_p \varphi_1}{P_a M_{a1} C_c}$$

$$K_2 = \frac{1.25 g K_j}{g + d_s}$$

$$K_3 = \frac{(b \pm 2bs) P M_{a1}}{B} \pm C_s M_s .$$

Use + $2b_s$ for brush shift in direction of rotation.

Use + $C_s M_s$ for differential field.

Partial compensation factor:

$$C_c = 1 - \frac{P_p}{P_a} \frac{M_{b1}}{M_{a1}}$$

$$r_b = E_r \ (1 - E_c) \ b \left(\frac{\varepsilon^x + 1}{\varepsilon^x - 1} \right) + V_c, \tag{11}$$

where $x = \dfrac{E_r \ (1 - E_c) \ b}{V_c}$.

Decrement factors:

$$\sigma_a = \frac{r_d'}{L_a} \tag{12}$$

$$\sigma_f = \frac{r_f}{L_f} \ . \tag{13}$$

* * *

APPENDIX II

OSCILLOGRAMS OF EXPERIMENTAL RESULTS
(Figures 29 through 47)

These oscillograms present current and voltage traces for submarine operating conditions as follows:

(a) Straight diesel electric drive - Figures 29 through 37.

(b) Diesel electric drive with batteries on charge - Figures 38 through 42.

(c) Submerged conditions, motors operating off the battery - Figures 43 through 47.

* * *

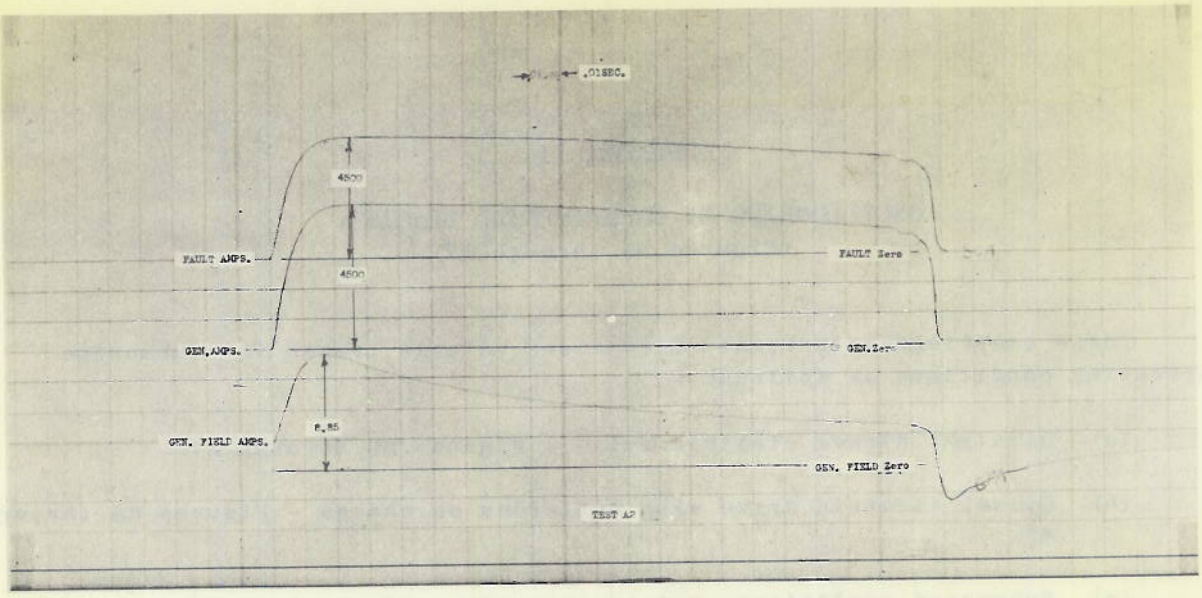

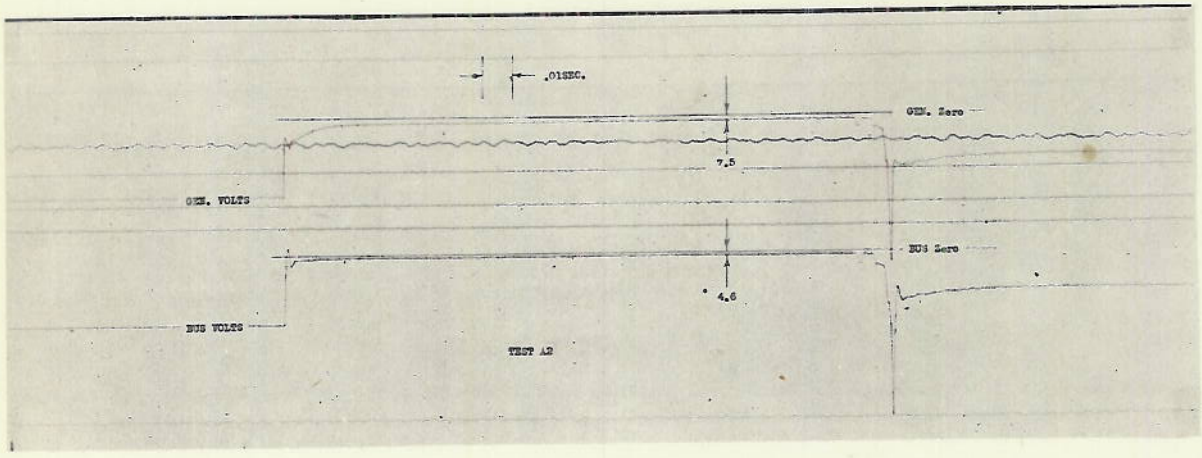

Figure 29 - Straight diesel electric drive - low-resistance fault. Initial conditions - generator: 110 V, no load. 720 rpm

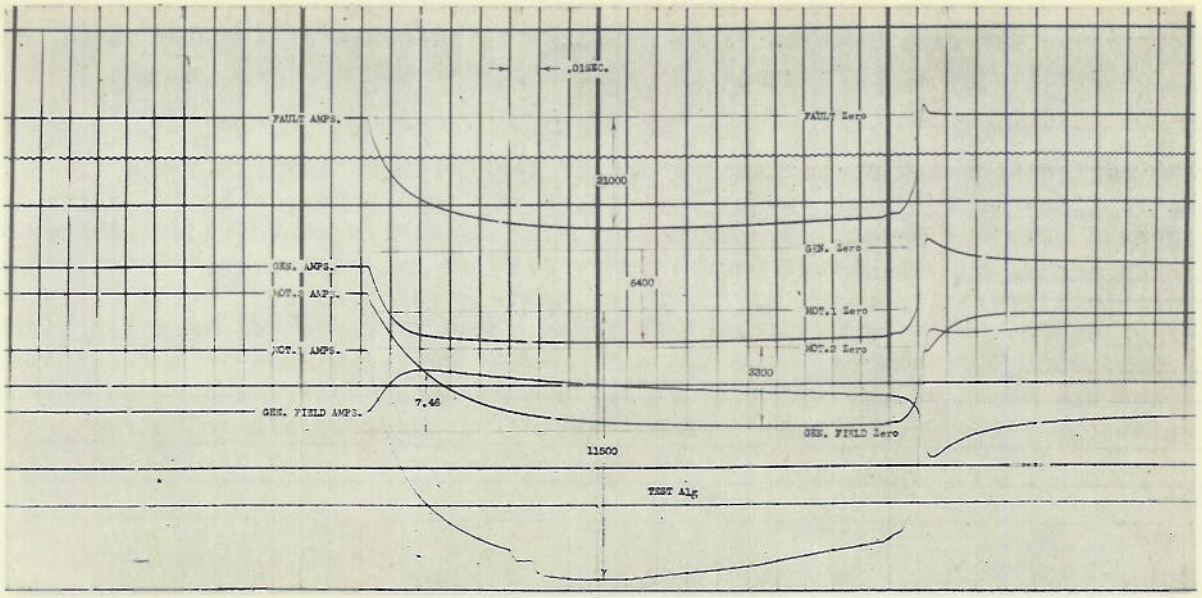

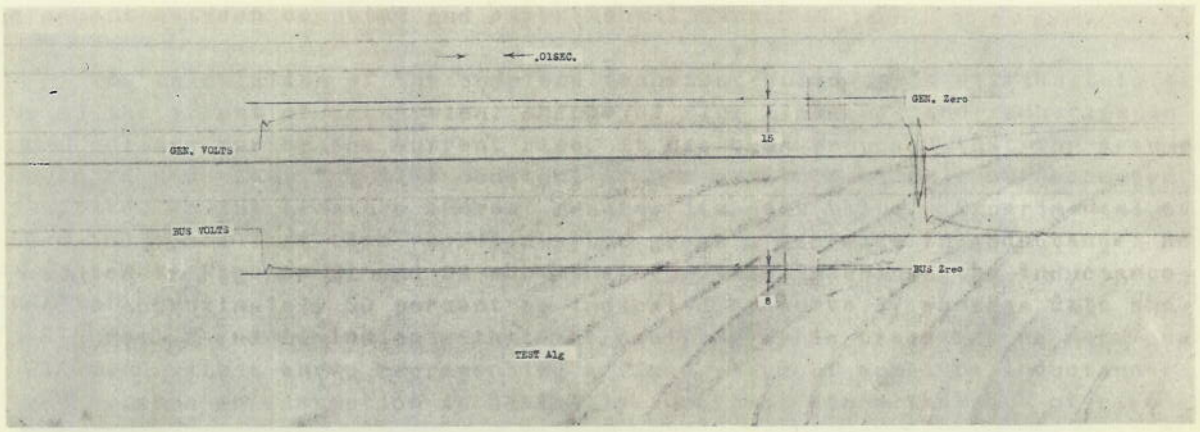

Figure 30 - Straight diesel electric drive - low-resistance fault.
Initial conditions - Generator: 111 V, 850 A, 619 rpm
Motor 1: 114 V, 1600 A, 684 rpm, generator action
Motor 2: 106 V, 2450 A, 148 rpm, motor action

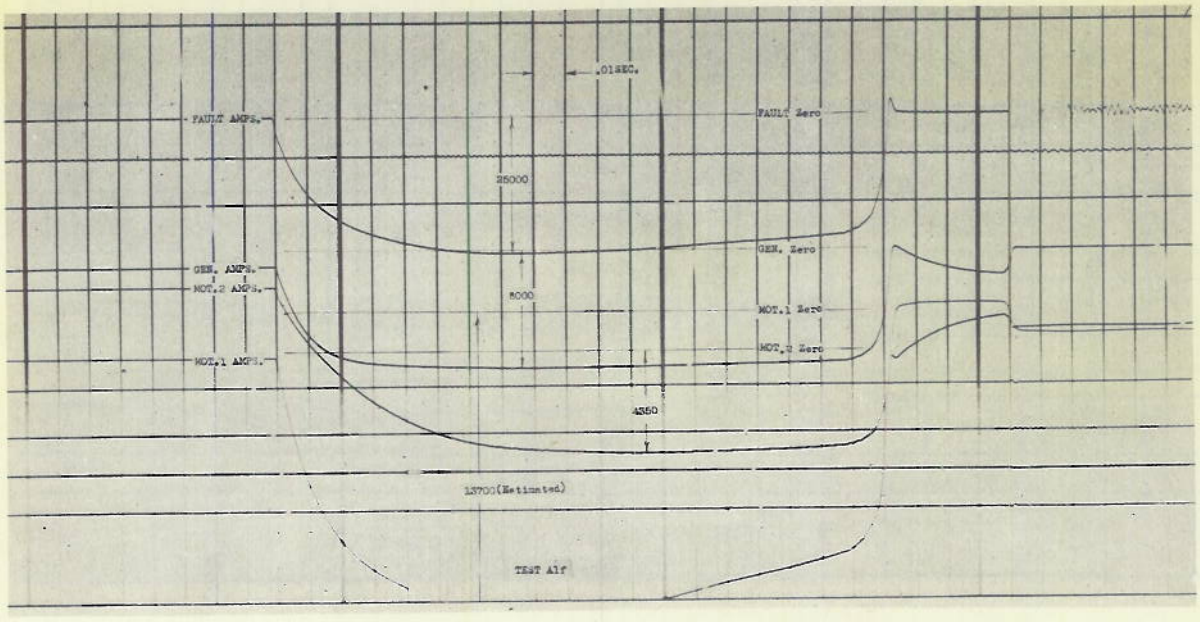

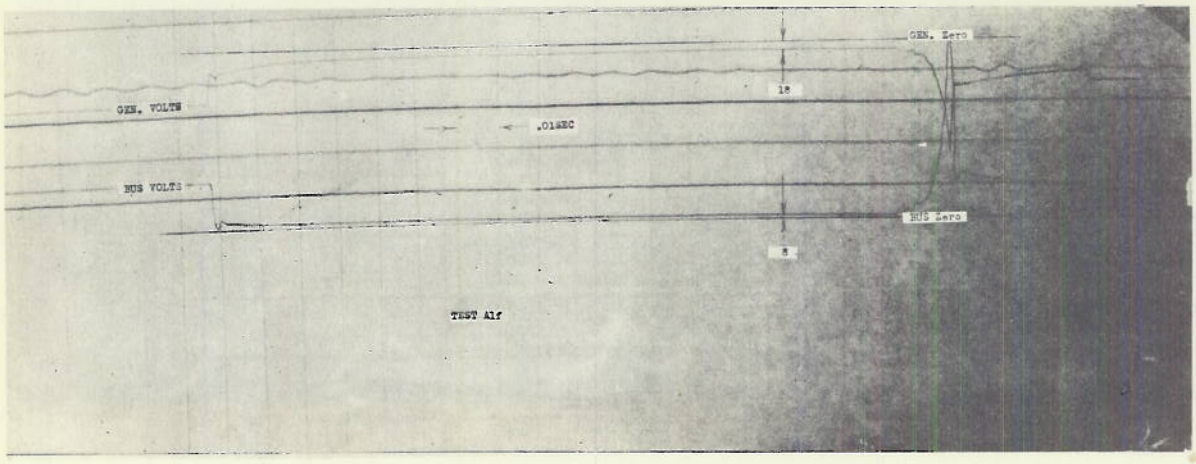

Figure 31 - Straight diesel electric drive - low-resistance fault.
Initial conditions - Generator: 111 V, 800 A, 428 rpm
Motor 1: 113 V. 1800 A, 428 rpm, generator action
Motor 2: 105 V, 2650 A, 92 rpm, motor action

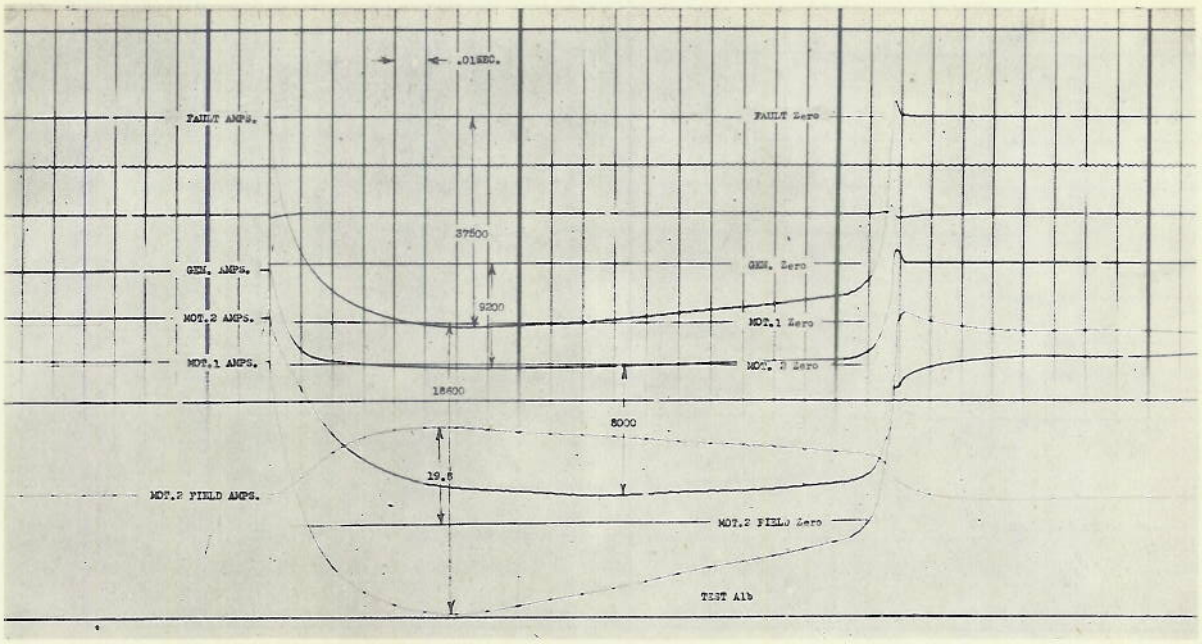

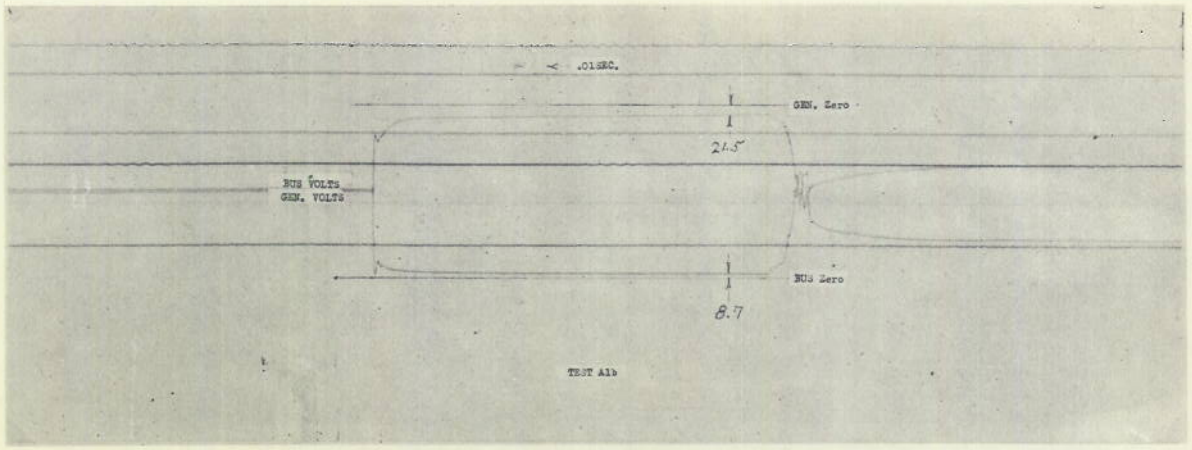

Figure 32 - Straight diesel electric drive - low-resistance fault.
Initial conditions - Generator: 202 V, 600 A, 710 rpm
Motor 1: 206 V, 2200 A, 638 rpm, generator action
Motor 2: 195 V, 2800 A, 137 rpm, motor action

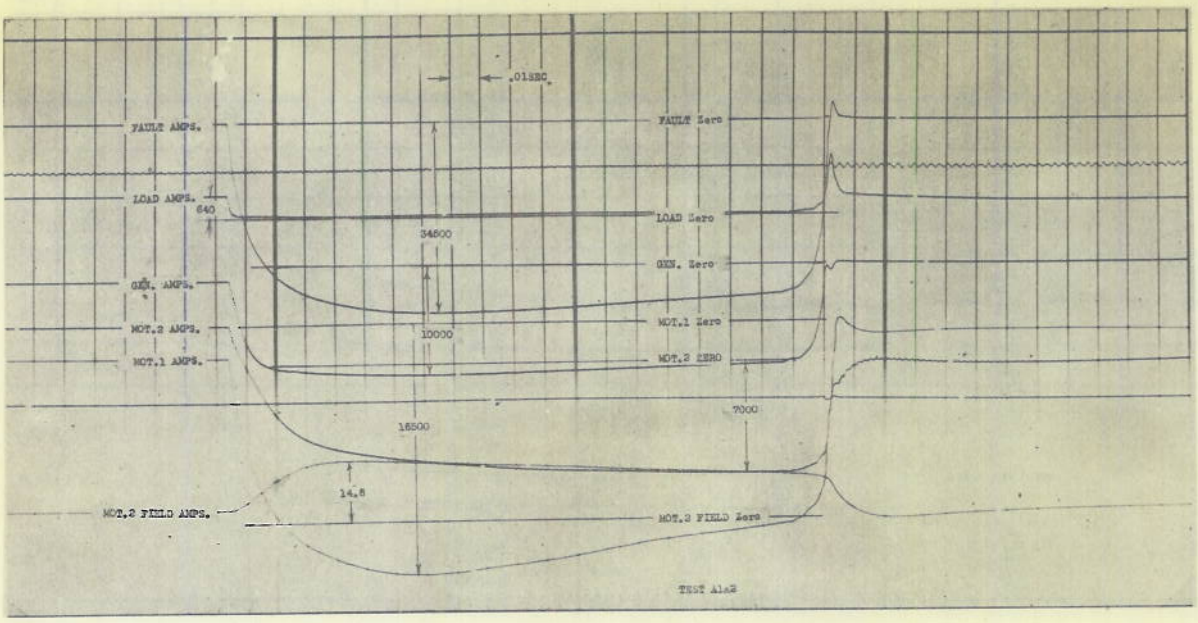

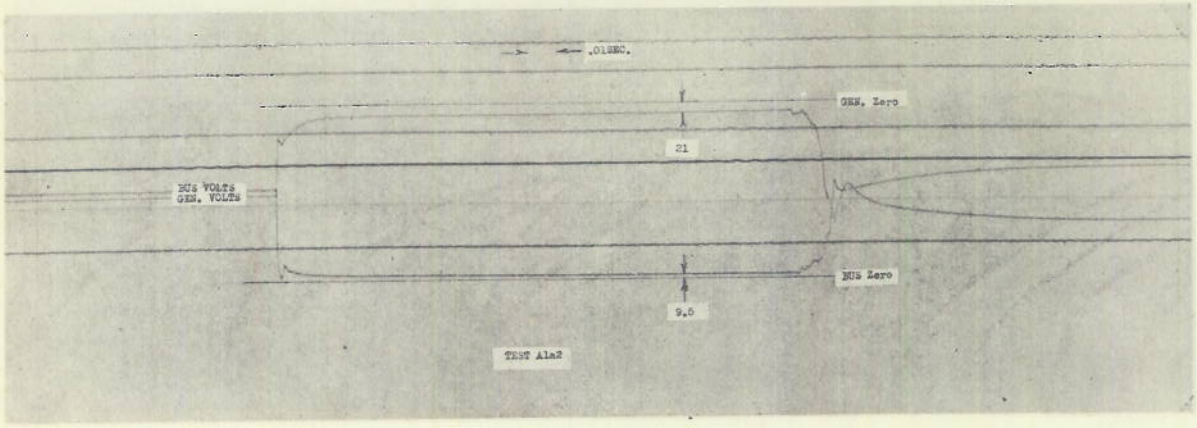

Figure 33 - Straight diesel electric drive - low-resistance fault.
Initial conditions - Generator: 202 V, 1200 A, 715 rpm
Motor 1: 200 V, 1900 A, 950 rpm, generator action
Motor 2: 190 V, 2500 A, 205 rpm, motor action

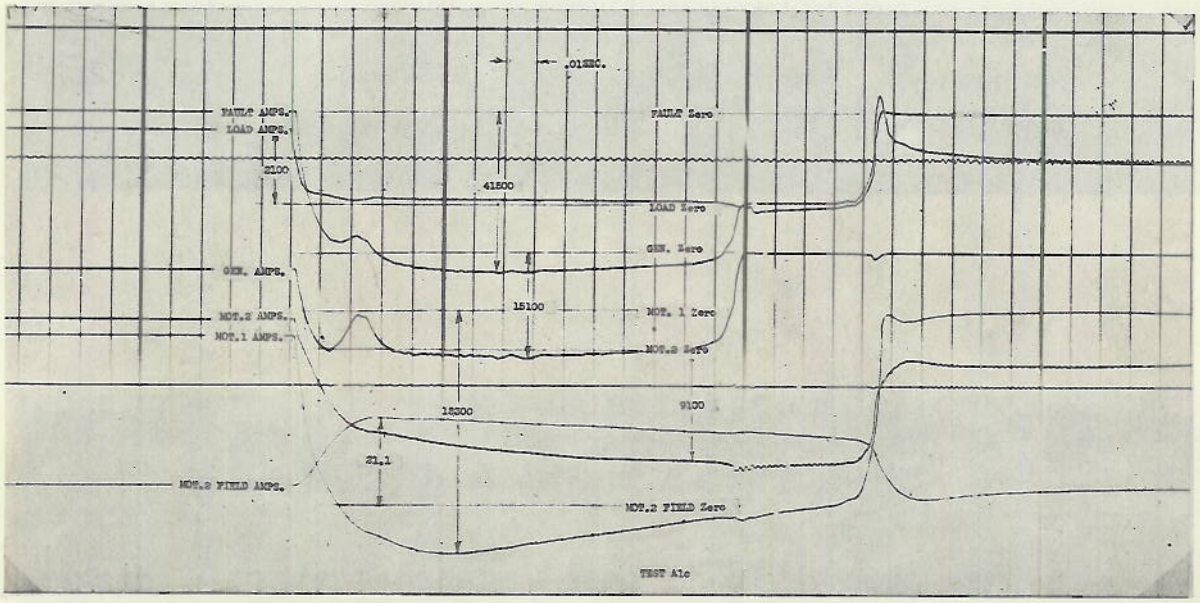

Figure 34 - Straight diesel electric drive - low-resistance fault.
Initial conditions - Generator: 304 V, 2600 A, 715 rpm
Motor 1: 303 V, 2000 A, 1238 rpm, generator action
Motor 2: 294 V, 2400 A, 267 rpm, motor action
(No voltage traces obtained.)

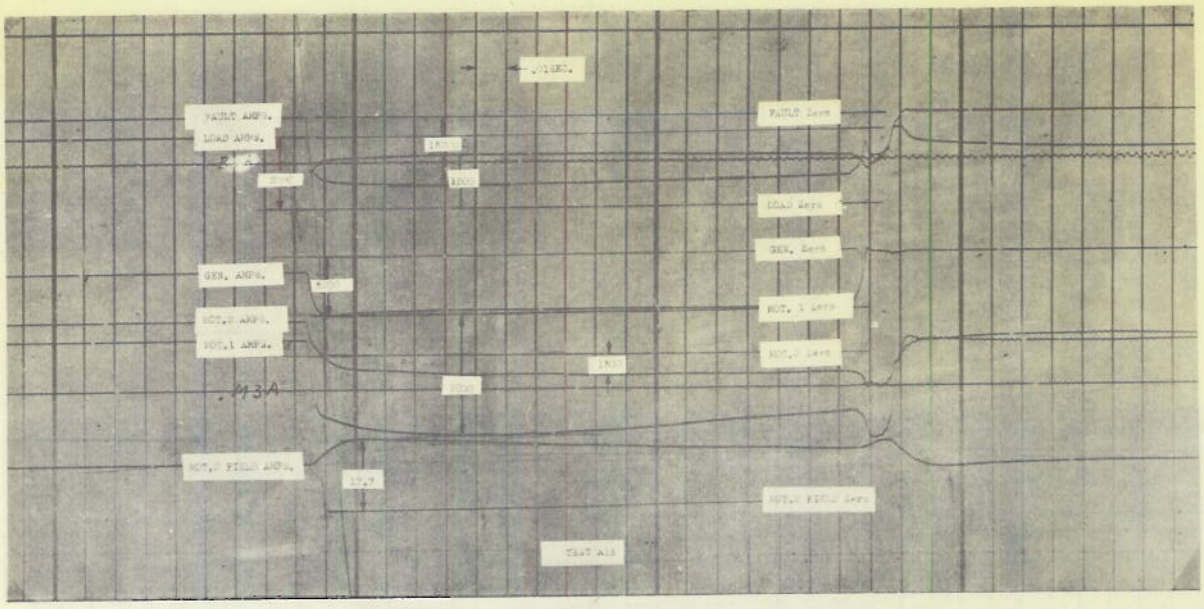

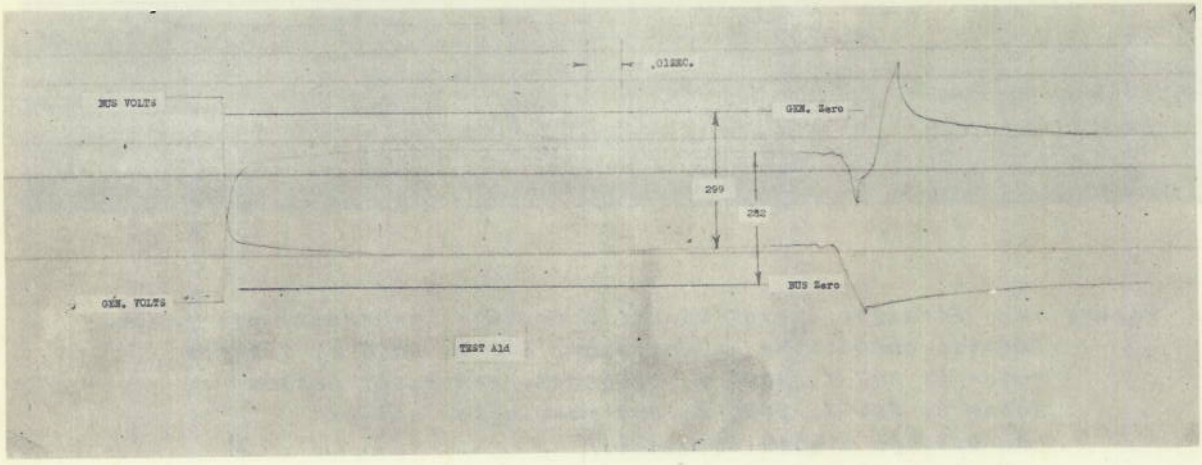

Figure 35 - Straight diesel electric drive - high-resistance fault.
Initial conditions - Generator: 419 V, 2300 A, 715 rpm
Motor 1: 419 V, 2200 A, 1255 rpm, generator action
Motor 2: 410 V, 2600 A, 270 rpm, motor action

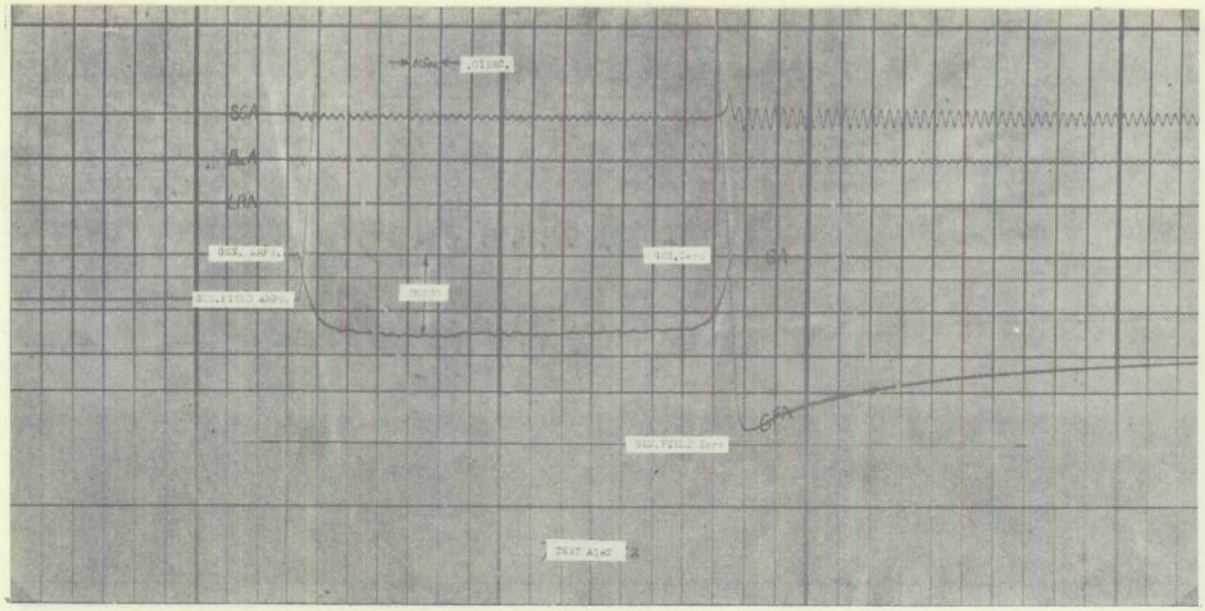

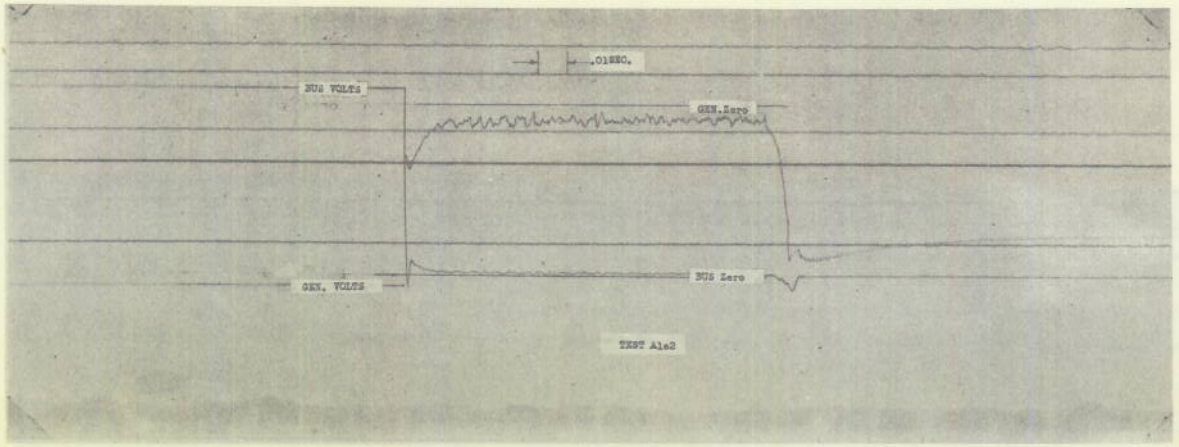

Figure 36 - Straight diesel electric drive - low-resistance fault. Initial conditions - Generator: 415 V, zero A, 715 rpm

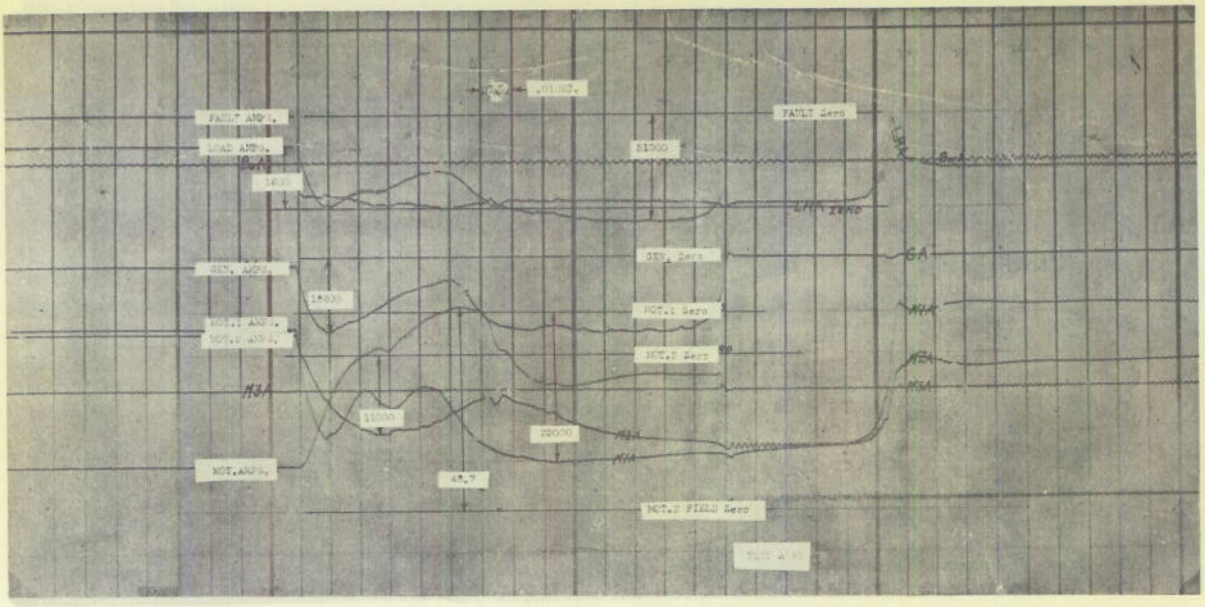

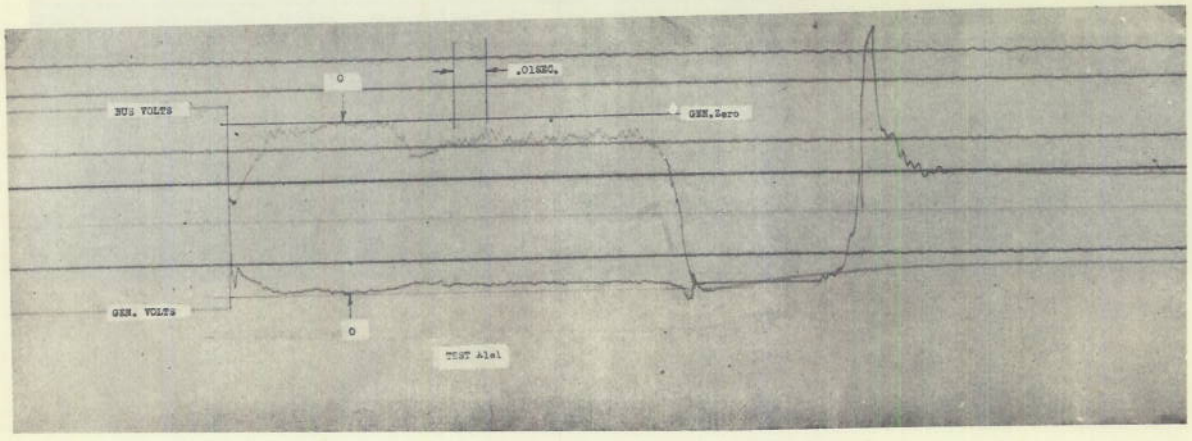

Figure 37 - Straight diesel electric drive - low-resistance fault.
Initial conditions - Generator: 418 V, 2000 A, 715 rpm
Motor 1: 417 V, 2300 A, 1238 rpm, generator action
Motor 2: 406 V, 2700 A, 267 rpm, motor action

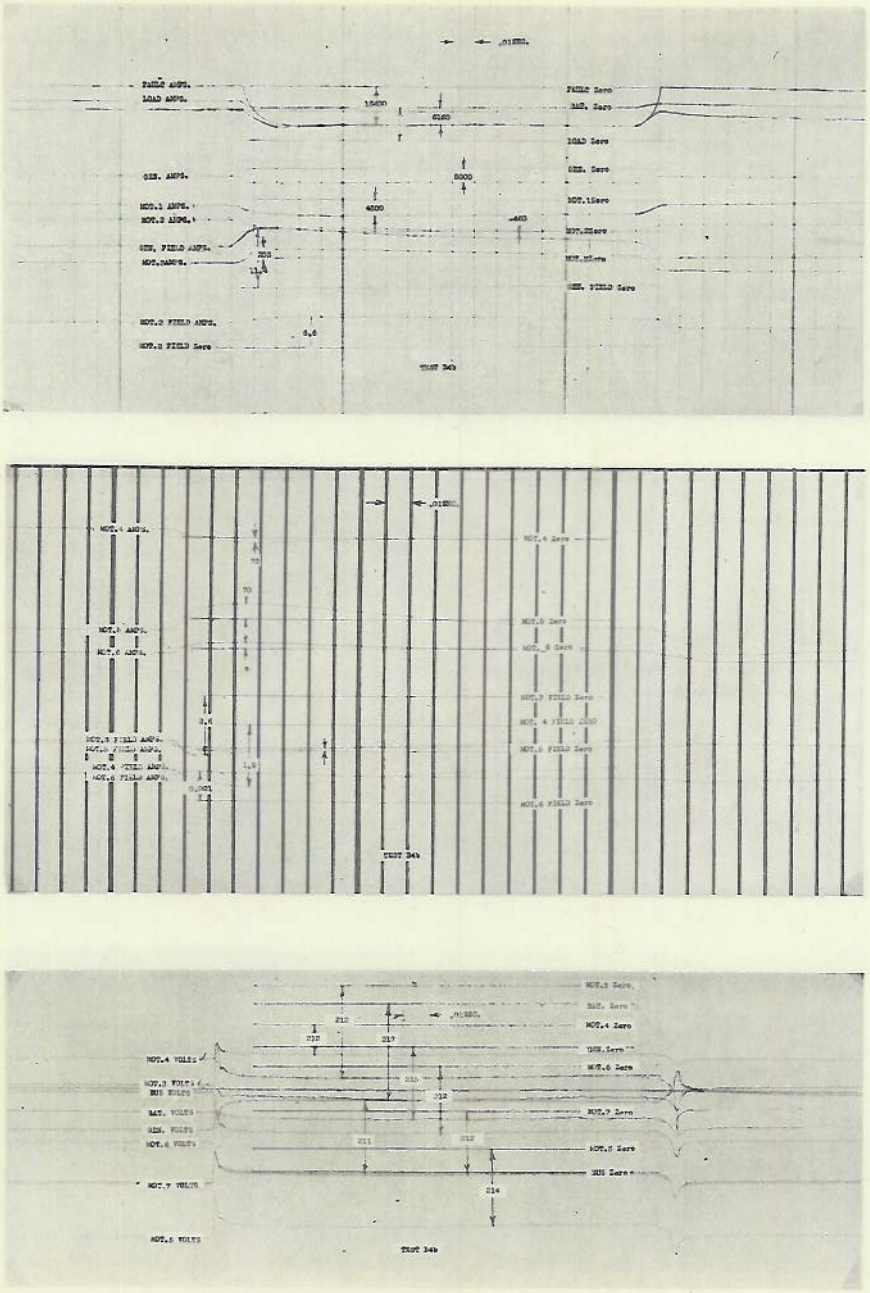

Figure 38 - Diesel electric drive with batteries on charge; high-resistance fault. Initial conditions -
Generator: 267 V, 2400 A, 704 rpm
Motor 1: 266 V, 2000 A, 1068 rpm, generator action
Motor 2: 258 V, 2450 A, 229 rpm, motor action
Motor 3: 260 V, 260 A, 1725 rpm
Motor 4: 260 V, 185 A, 530 rpm
Motor 5: 261 V, 40 A, 1900 rpm
Motor 6: 261 V, 0.7 A, 1562 rpm
Motor 7: 260 V, 0.2 A, 2100 rpm
Battery: 261 V, float condition

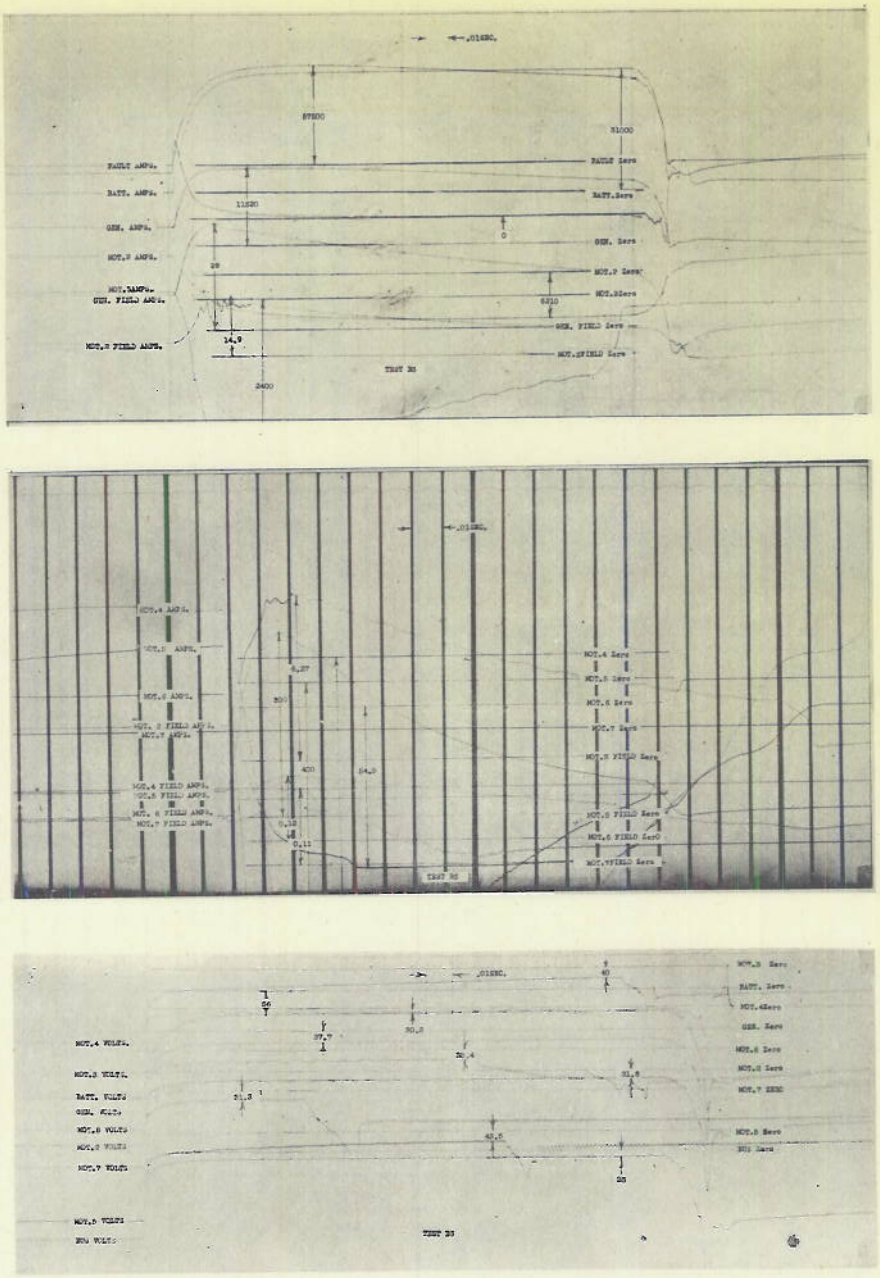

Figure 39 - Diesel electric drive with batteries on charge; low-resistance fault. Initial conditions-
Generator: 268 V, 2625 A, 720 rpm
Motor 1: 266 V, 2000 A, 1280 rpm, generator action
Motor 2: 260 V, 2510 A, 276 rpm, motor action
Motor 3: 254 V, 195 A, 1800 rpm
Motor 4: 250 V, 118 A, 530 rpm
Motor 5: 264 V, 31 A, 1930 rpm
Motor 6: 258 V, 4.1 A, 1650 rpm
Motor 7: 261 V, 0.14 A, 2400 rpm
Battery: 250 A, (charge)

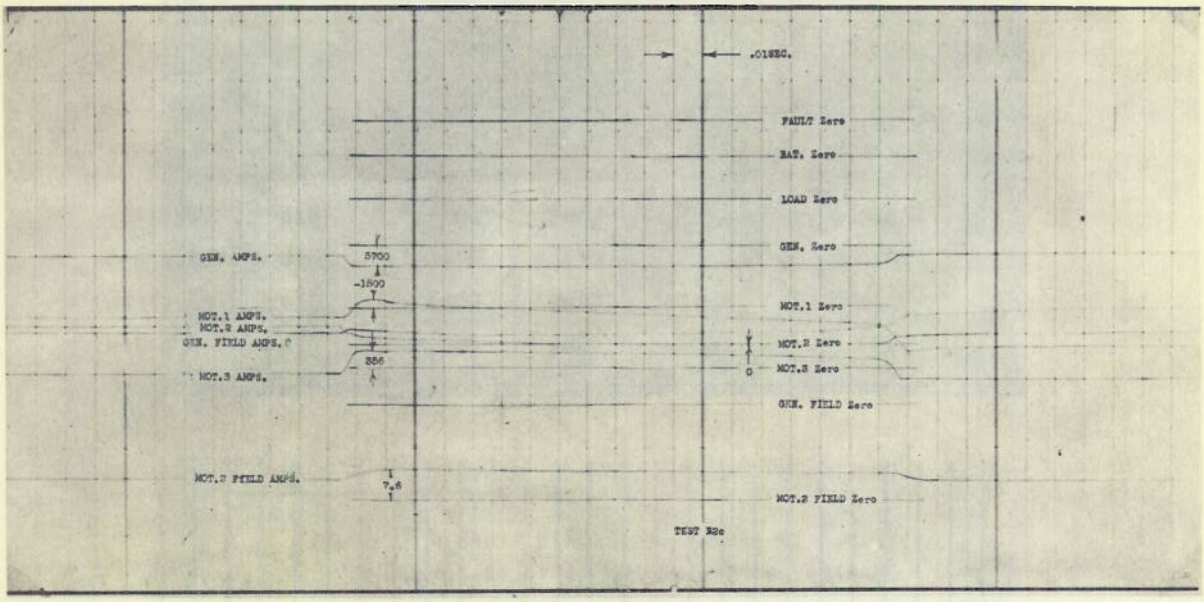

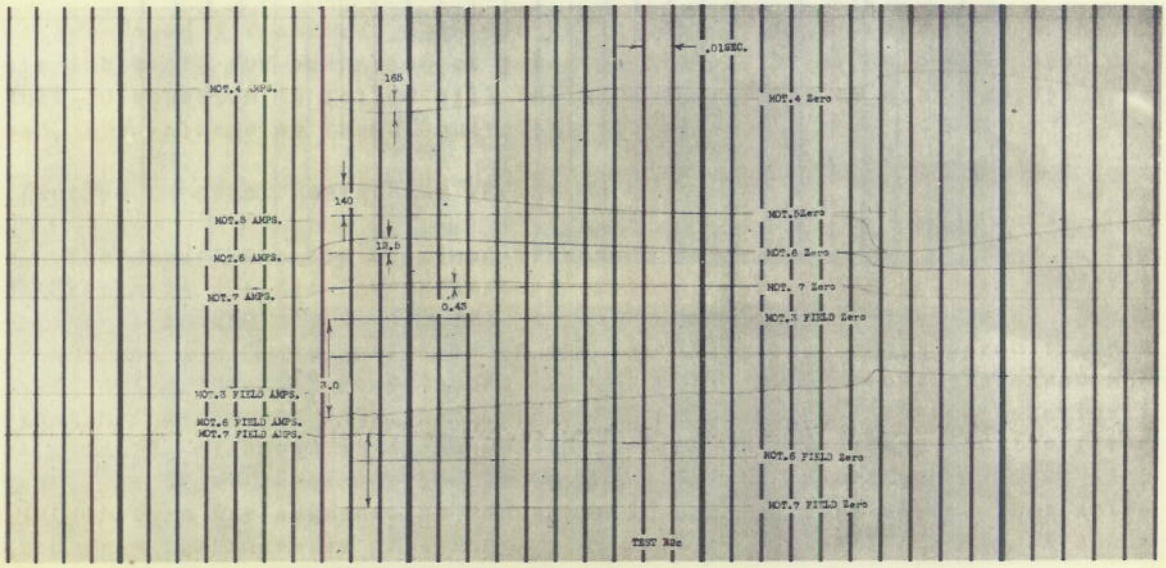

Figure 40 - Diesel electric drive with batteries on charge; high-resistance fault. Initial conditions -
Generator: 323 V, 2400 A, 715 rpm
Motor 1: 322 V, 2050 A, 1275 rpm, generator action
Motor 2: 316 V, 2500 A, 275 rpm, motor action
Motor 3: 318 V, 130 A, 2000 rpm
Motor 4: 318 V, 150 A, 486 rpm
Motor 5: 318 V, 18 A, 1855 rpm
Motor 6: 318 V, 0.42 A, 1532 rpm
Motor 7: 318 V, 0.14 A, 2240 rpm
Battery: 318 V, 300 A, (charge)

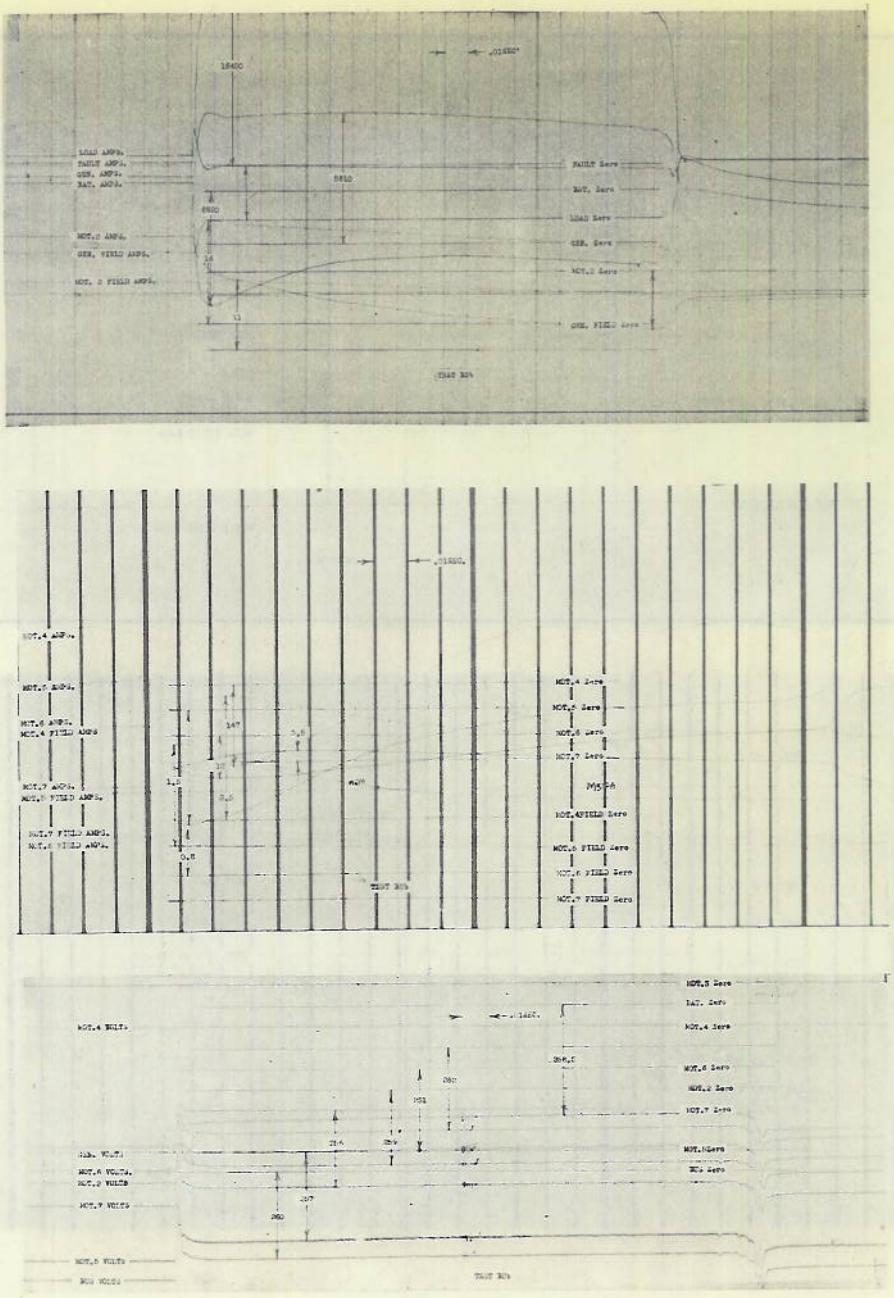

Figure 41 - Diesel electric drive with batteries on charge; high-resistance fault. Initial conditions-
Generator: 338 V, 3080 A, 750 rpm
Motor 1: 338 V, 1400 A, 1320 rpm, generator action
Motor 2: 328 V, 1560 A, motor action
Motor 3: Not running
Motor 4: 330 V, 123 A, 540 rpm
Motor 5: 333 V, 24 A, 2020 rpm
Motor 6: 329 V, 3.12 A, 1650 rpm
Motor 7: 333 V, 0.84 A, 2500 rpm
Battery: 332 V, 350 A, (charge)

Note: motor 2 cumulative-compounded for generator action

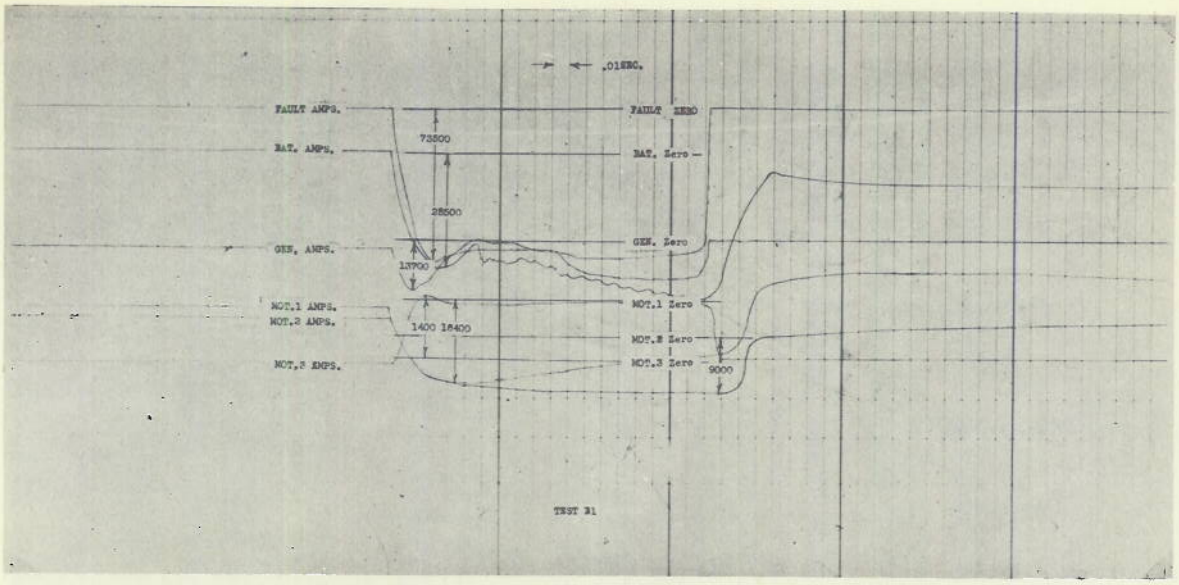

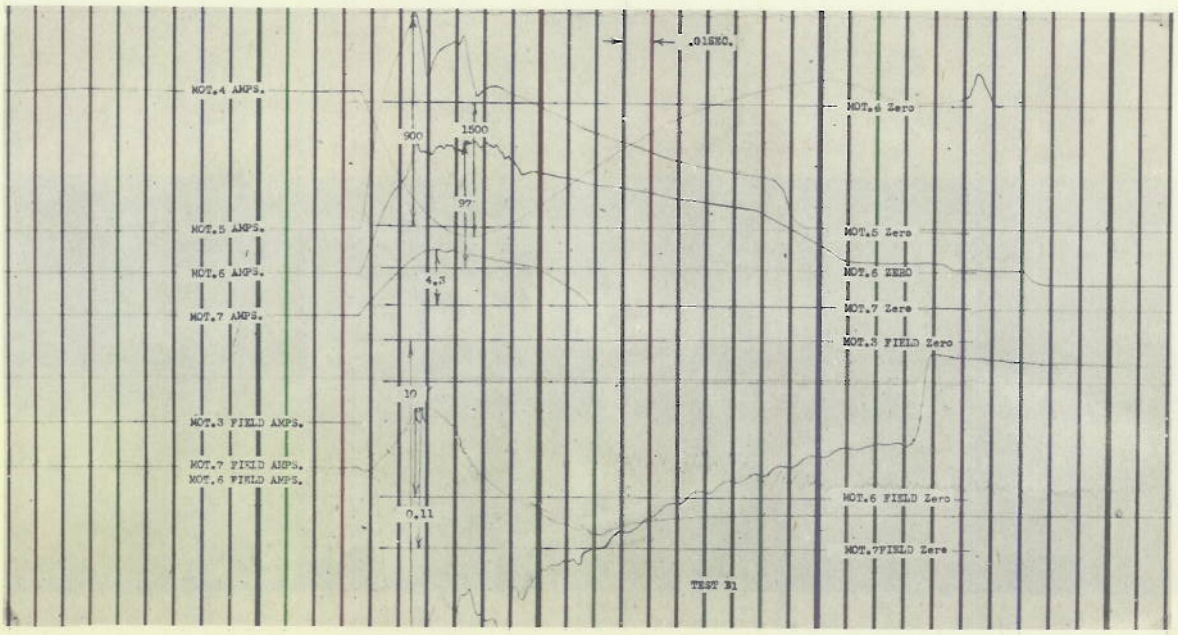

Figure 42 - Diesel electric drive with batteries on charge; low-resistance fault. Initial conditions-
Generator: 322 V, 2400 A, 695 rpm
Motor 1: 323 V, 2000 A, 1258 rpm, generator action
Motor 2: 314 V, 2500 A, 270 rpm, motor action
Motor 3: 316 V, 130 A, 1580 rpm
Motor 4: 318 V, 147 A, 514 rpm
Motor 5: 318 V, 18 A, 2095 rpm
Motor 6: 318 V, 0.42 A, 1570 rpm
Motor 7: 318 V, 0.14 A, 2380 rpm
Battery: 330 A, (discharge)

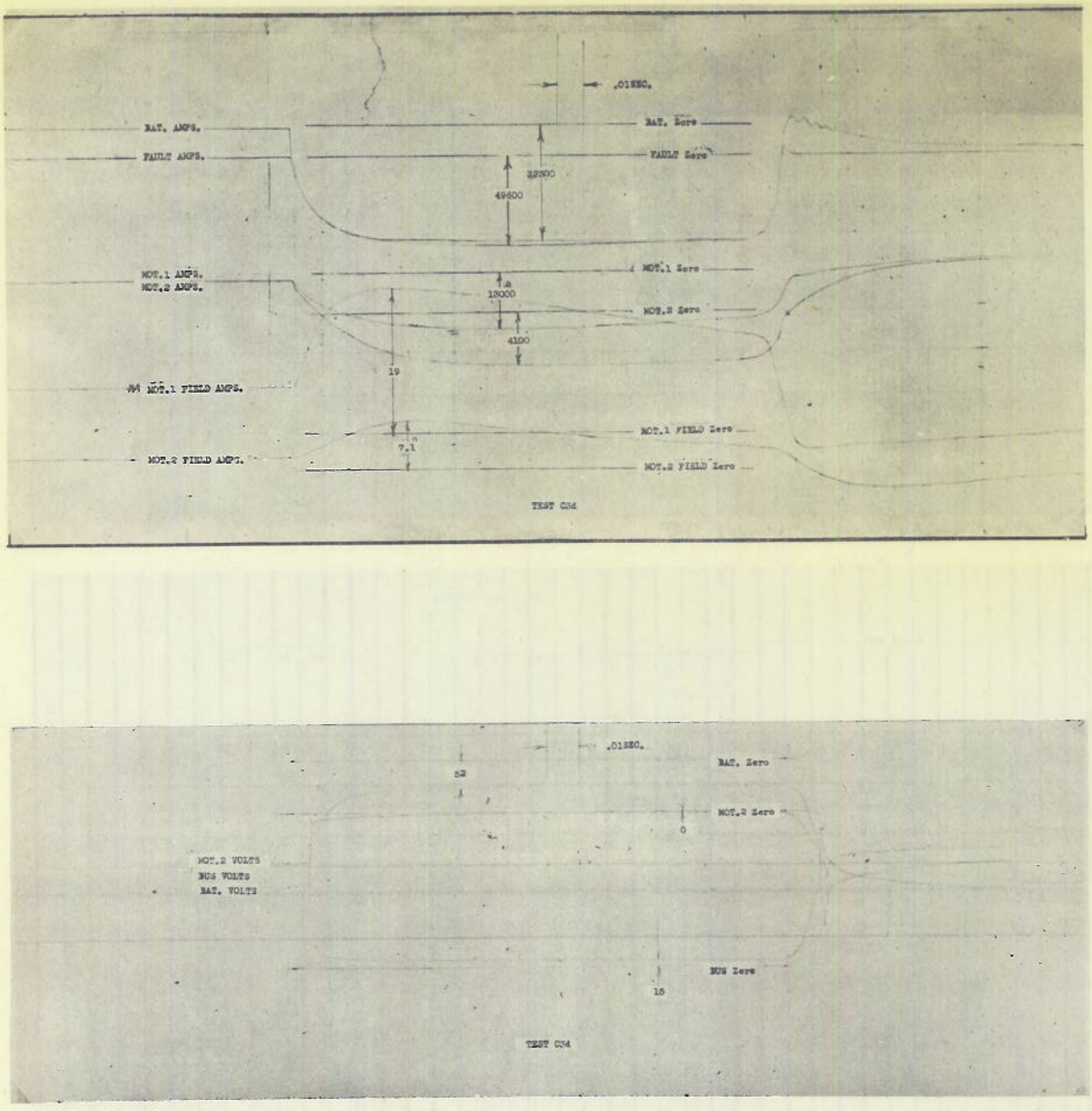

Figure 43 - Submerged conditions - low-resistance fault.
Initial conditions -
Motor 1: 120 V, 1750 A, 715 rpm, generator action
Motor 2: 117 V, 2500 A, 154 rpm, motor action
Battery: 750 A, (discharge)

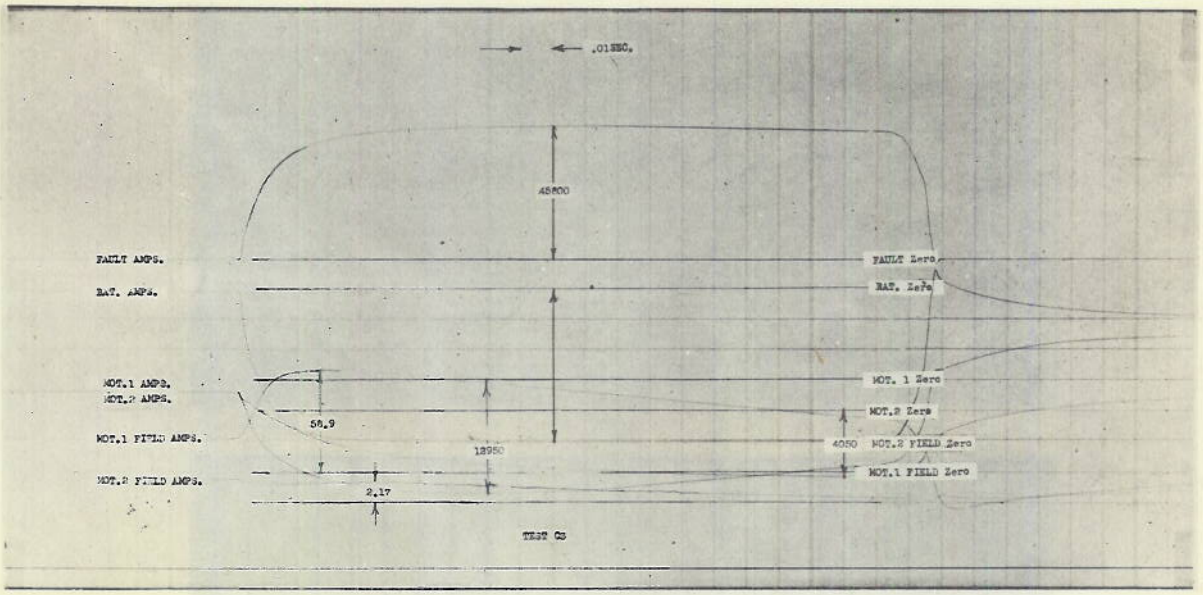

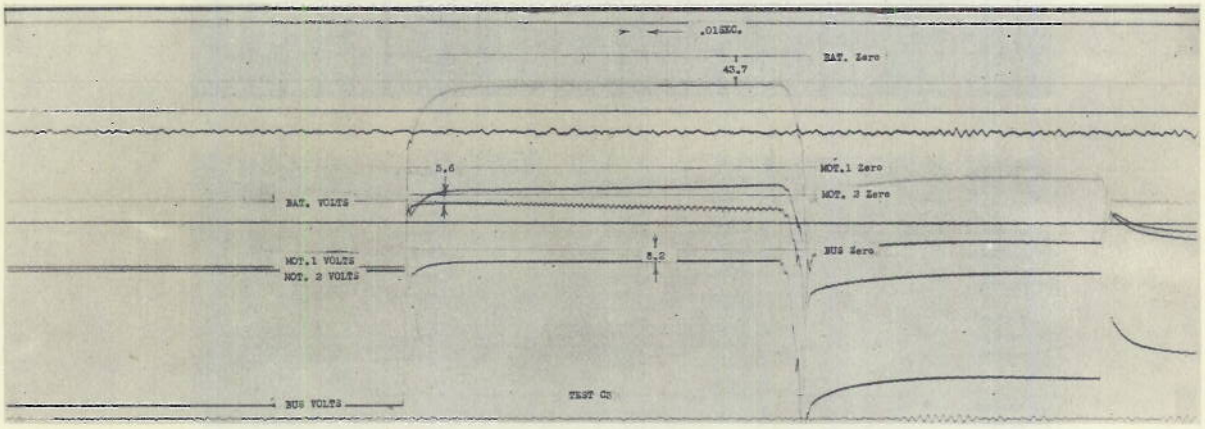

Figure 44 - Submerged conditions - low-resistance fault.
Initial conditions -
Motor 1: 125 V, 1720 A, 418 rpm, generator action
Motor 2: 108.5 V, 2510 A, 90 rpm, motor action
Battery: 823 A, (discharge)

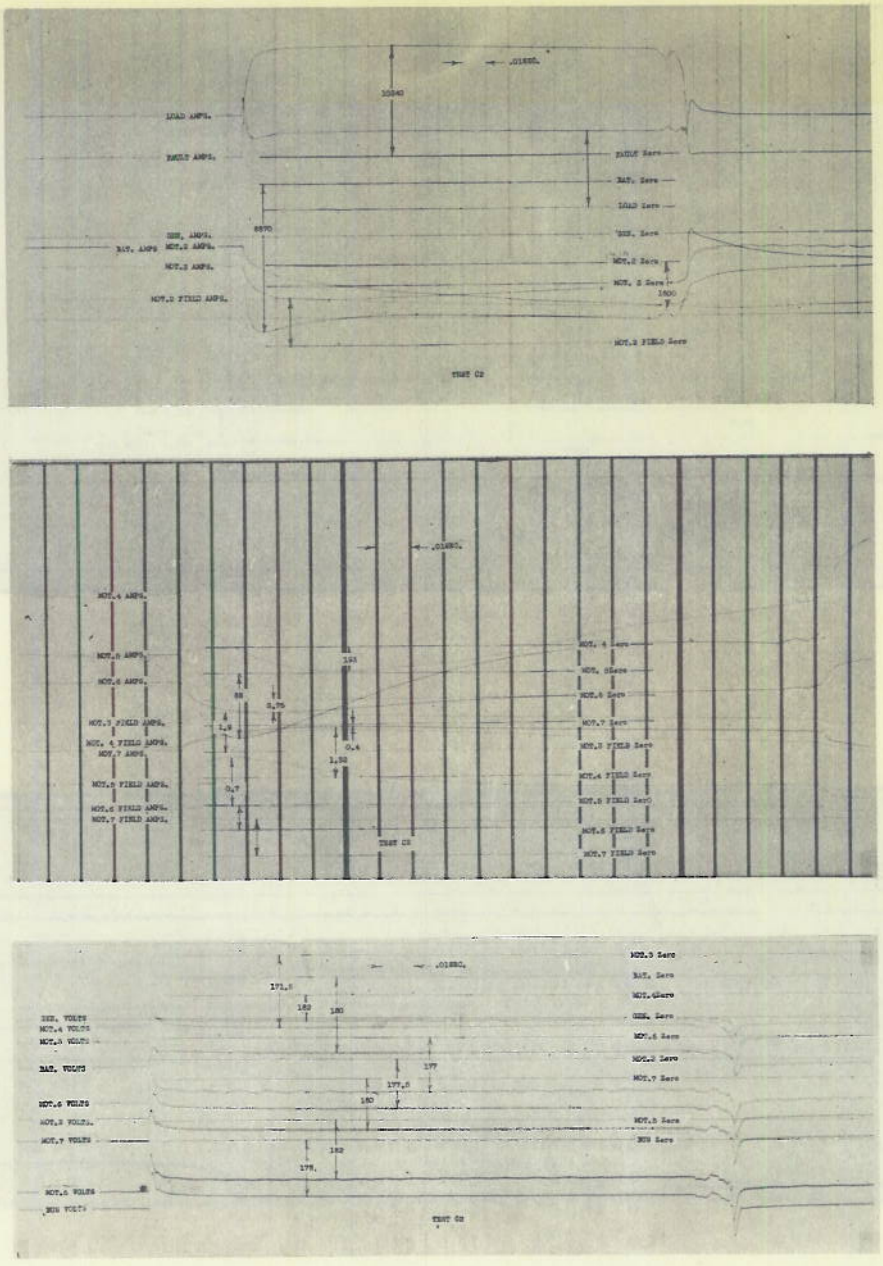

Figure 45 - Submerged conditions - high-resistance fault.
Initial conditions:
Motor 1: 250 V, 2000 A, 1050 rpm, generator action
Motor 2: 222 V, 2550 A, 226 rpm, motor action
Motor 3: 224 V, 110 A, 1580 rpm
Motor 4: 224 V, 145 A, 477 rpm
Motor 5: 234 V, 31 A, 1810 rpm
Motor 6: 224 V, 110 A, 1505 rpm
Motor 7: 204 V, 1.1 A, 2140 rpm
Battery: 3400 A, (discharge)

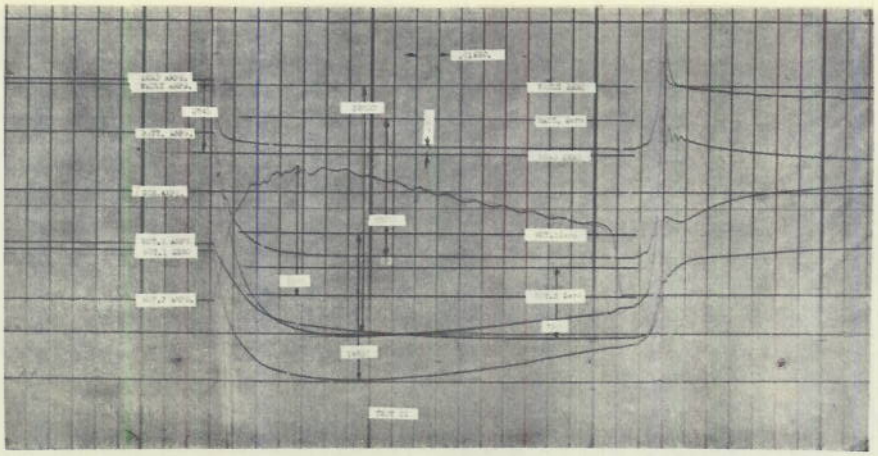

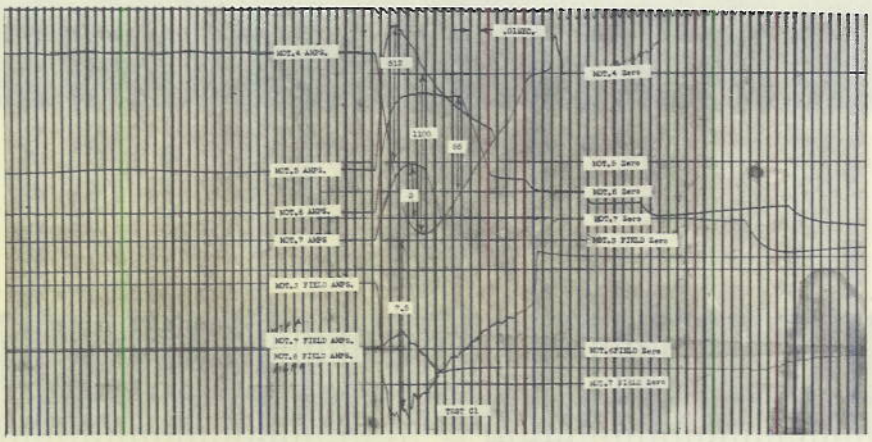

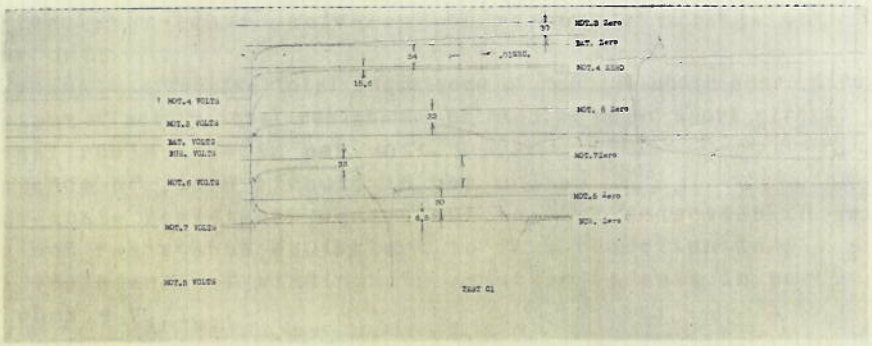

Figure 46 - Submerged conditions - low-resistance fault.

Initial conditions:

Motor 1: 229 V, 1650 A, 1085 rpm, generator action

Motor 2: 221 V, 2200 A, 234 rpm, motor action

Motor 3: 224 V, 110 A, 1600 rpm

Motor 4: 223 V, 192 A, 482 rpm

Motor 5: 223 V, 25 A, 1845 rpm

Motor 6: 233 V, 12.5 A, 1600 rpm

Motor 7: 224 V, 1.2 A, 2095 rpm

Battery: 3400 A, (discharge)

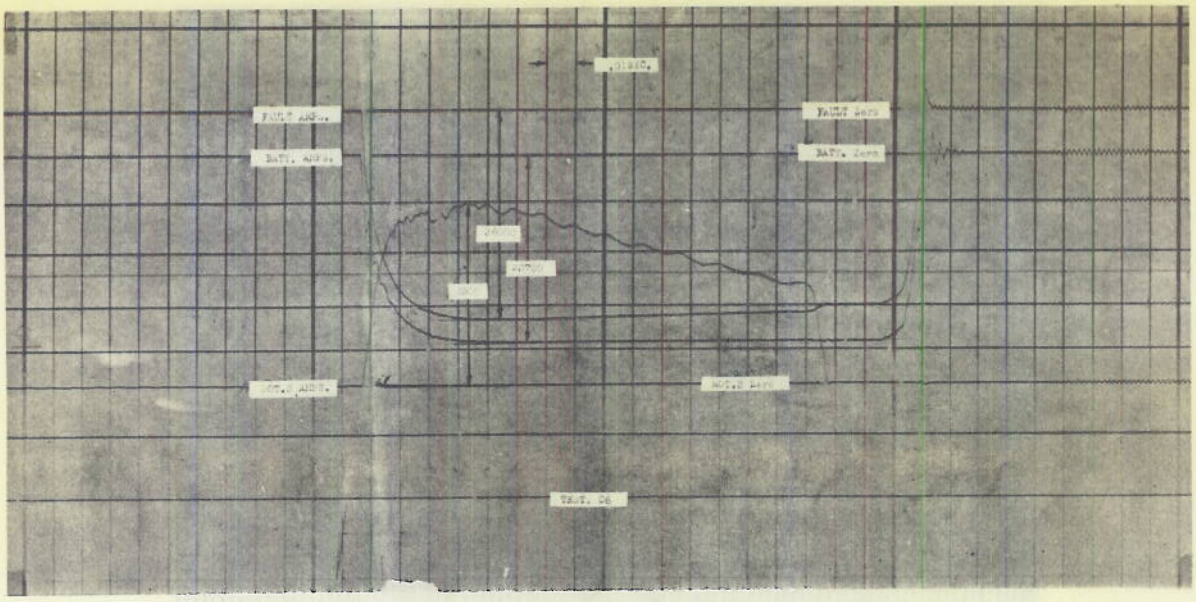

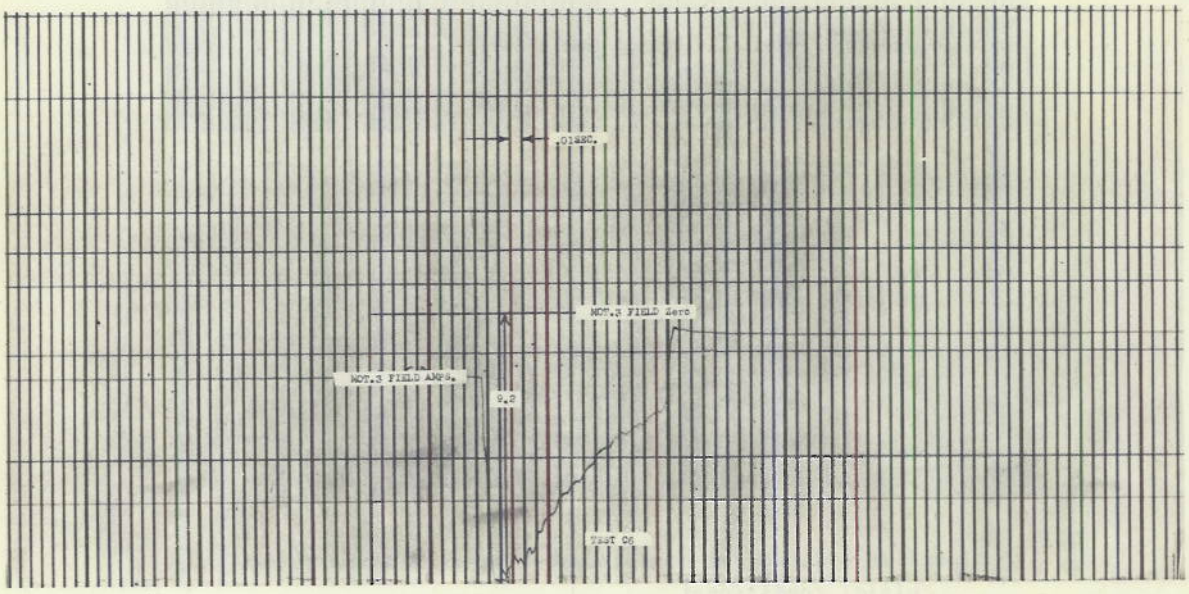

Figure 47 - Submerged conditions - low-resistance fault. Initial conditions - Motor 3: 259 V, 15 A, 1800 rpm

SYMBOLS

b = brush overlap in segments.
b_s = brush shift from polar axis in segments.
B = total number of segments in commutator.
d_s = depth of armature slot in inches.
E_c = estimated ratio (under sustained short circuit conditions) of actual interpole field strength to field strength if no saturation occurred. (Generalized value = 0.3)
e_o = armature emf before short circuit in per unit.
E_r = average per-unit reactance voltage per coil at rated full-load current.
g = average main pole air gap in inches.
i_a = instantaneous short circuit current in per unit.
i_f = instantaneous short circuit field current in per unit.
I_a' = maximum short circuit in per unit. (Based on rated current.)
K_i = air gap plus tooth ampere turns divided by air gap ampere turns at rated voltage, base rated speed, no load.
L_f = inductance of field circuit divided by unit ohms (R_1).
M_{a1} = armature reaction mmf. at full rated load in per unit.
M_{f1} = base ampere turns = field ampere turns per pole at rated voltage, rated base speed, no load.
n_f = ratio total field flux linkages minus linkages from flux responsible for armature emf to linkages from flux responsible for armature emf.
n_o = speed at which machine is short circuited in per unit.
P_a = pole arc in inches.
P_p = pole pitch in inches.
P = number of poles.
r_b = steady-state resistance equivalent to reactance voltage and brush contact in per unit.
r_b' = transient resistance equivalent to reactance voltage and brush contact in per unit.
r_d = steady-state effective total resistance of machine under short circuit in per unit.
r_d' = transient effective total resistance of machine under short circuit in per unit.
r_e = external resistance in per unit.
r_f = resistance of field circuit in per unit.
r_x = steady-state resistance equivalent to flux reduction in per unit.
r_x' = transient resistance equivalent to flux reduction in per unit.
r_w = total resistance of windings in armature circuit in per unit.
R_1 = base ohms = V_1/I_{a1}.
V_1 = base volts = rated voltage in volts.
V_c = normal brush contact drop at full load in per unit.
φ_1 = base flux = flux per pole in maxwells at rated voltage, rated base speed, no load.
φ_1 = iron flux per pole in per unit = average section of armature tooth in sq. in. times number of teeth in pole arc x 123,000 lines per sq. in. divided by φ_1.
σ_a = armature circuit decrement factor.
σ_f = field circuit decrement factor.
C_s = series field coupling factor.
M_s = series field ampere turns, in per unit.
M_{b1} = compensating winding ampere turns on pole face, in per unit.

NAVY-DPPO PRNC. WASH., D.C.